Accepted Article

Title: Production of cycloalkanes in hydrodeoxygenation of isoeugenol over Pt- and Ir-modified bifunctional catalysts

Authors: Louis Bomont, Moldir Alda-Onggar, Vyacheslav Fedorov, Atte Aho, Janne Peltonen, Kari Eränen, Markus Peurla, Narendra Kumar, Johan Wärnå, Vincenzo Russo, Päivi Mäki-Arvela, Henrik Grenman, Marina Lindblad, and Dmitry Murzin

WILEY-VCH

Production of cycloalkanes in hydrodeoxygenation of isoeugenol over Pt- and Ir-modified bifunctional catalysts

Louis Bomont[a], Moldir Alda-Onggar[a], Vyacheslav Fedorov[a], Atte Aho[a], Janne Peltonen[b], Kari Eränen[a], Markus Peurla[c], Narendra Kumar[a], Johan Wärnå[a], Vincenzo Russo, [d] Päivi Mäki-Arvela[a], Henrik Grénman[a], Marina Lindblad[e], Dmitry Yu. Murzin[a*]

[a]*Johan Gadolin Process Chemistry Centre, Åbo Akademi University, Turku/Åbo, Finland*

[b]*Laboratory of Industrial Physics, University of Turku, Turku, Finland*

[c]*Laboratory of Electron Microscopy, University of Turku, Finland*

[d] *Università di Napoli Federico II. Via Cinthia, 4. IT-80126 Napoli, Italy*

[e] *Neste Corporation, Porvoo, Finland*

corresponding author: dmurzin@abo.fi, web page: http://users.abo.fi/dmurzin/

Hydrodeoxygenation of isoeugenol was investigated at 200°C under 3 MPa total pressure in dodecane as a solvent in hydrogen over bifunctional Pt- and Ir-modified beta zeolites and mesoporous materials. As a comparison, also Pt- and Ir-supported on Al_2O_3, SiO_2 and mesoporous MCM-41 were tested. The catalysts were characterized by XRD, CO pulse chemisorption, transmission electron microscopy, scanning electron microscopy, nitrogen adsorption and FTIR pyridine adsorption desorption. The results revealed that the most active and selective catalyst was Pt-H-Beta-300 exhibiting the lowest acidity and largest crystal size of Beta zeolite among the studied Pt- and Ir-modified Beta zeolites. Complete conversion of isoeugenol and 89% selectivity to propylcyclohexane was obtained with this catalyst in 240 min. The overall deoxygenation selectivity was 100% giving also dialkylated cyclohexanes as the second major product. This catalyst was also regenerated, reduced and reused in hydrodeoxygenation of isoeugenol showing nearly the same performance as the fresh one. Termodynamic analyses and kinetic modelling of the data were also performed for hydrodeoxygenation of isoeugenol.

Introduction

Pyrolysis of biomass and lignin extraction have been intensively studied for production of bio-oil and lignin fractions. [1-4] Phenolic compounds contain, however, still large amounts of oxygen not being suitable for a direct use as fuels, thus these compounds have been deoxygenated over various catalysts. Hydrodeoxygenation (HDO) of phenolic compounds is not very easy due to strong adsorption of multioxygenated compounds on the catalyst surface causing also coking and catalyst deactivation. Moreover, repolymerisation of phenolic compounds at higher reaction temperatures is still feasible resulting in lower catalyst activities and a lack of the liquid phase mass balance closure determined by GC. [5] In order to produce fully deoxygenated hydrocarbons, bifunctional catalysts are needed exhibiting both metal and acidic function.

Several model compounds, such as guaiacol, [5-13] anisole, [12, 14-15] and phenol [16] have been intensively used in HDO using different catalysts. HDO of eugenol has, however, been less intensively investigated. [17-27] It has already been shown that the main product was dihydroeugenol over Pt-alumina silicate at 250°C under 3 MPa, whereas more strongly acidic catalysts, such as $Ni-SiO_2-ZrO_2$ gave fully deoxygenated propylcyclohexane as the main product at 300°C under 5 MPa total hydrogen, when a mixture of phenol, cresol, eugenol, trans-anethole, vanillin and guaiacol was used as a feedstock. [19] Several very recent works in eugenol HDO show clearly that acidity is required for production of hydrocarbons [20, 21] and high temperatures using Ru/C as a catalyst. [22] Higher metal dispersions also promoted HDO as was the case with different Ru-supported catalysts. [23] In another work [18] a physical mixture of Pd/C with alkali leached mesoporous H-ZSM-5 gave in HDO of eugenol 73% hydrocarbons at 87% conversion at 250°C under 5 MPa hydrogen after 4 h showing a need of acidity. Hydrodeoxygenation of eugenol was also investigated over Raney nickel together with H-ZSM-5 at 220°C under 0.5 MPa nitrogen in methanol – water mixture. The main product was

2

propylcyclohexane with the yield of 86.1% after 7 h. [20] Nickel phosphide supported on HZSM-5 was giving at 250°C 60% conversion of eugenol after 2 h. The degree of product deoxygenation was 44% with propylcyclohexane being the main product. [24] Cobalt catalyst supported on HZSM-5 was active in eugenol HDO giving 100% conversion and 62% selectivity towards propylcyclohexane at 200°C under 1 MPa hydrogen in 2 h, whereas Co/CeO₂ resulted in only 14 % of this product. [25] High yields of propylcyclohexane, 90% were also reported in eugenol HDO over Ru/CNT catalyst at 220°C under 5 MPa hydrogen in 3 h using undecane water mixture as a solvent. [26] Ru/HZSM-5 as a catalyst gave 83% yield of propylcyclohexane in water at 170°C under 4 MPa hydrogen in 4 h. In this case the carbon balance was stated to be 91%. [21] On the other hand, Ru/MW-CNT produced only 28% propylcyclohexane when eugenol was transformed under 4 MPa hydrogen at 270°C in water as a solvent after 1 h. [23] It should be mentioned that the reaction time was, however, short and thus this result is not fully comparable with that of Wang et al. [21] Ru/C was used as a catalyst in eugenol HDO with hexadecane as a solvent showing that temperature above 275° C favored deoxygenation. [22] In minor amounts 1-methyl-3-ethylcyclohexane [20] and products of ring contraction such as alkylated cyclopentane [13] have been reported. In addition, skeletal isomerization of the side chain in main product is also possible forming isopropylcyclohexane.

Application of expensive noble methods with low loading is often done in oil refining for such processes as catalytic reforming, isomerisation and hydrocracking. Precious metal-containing catalysts are also used in production of bulk and specialty chemicals. Despite high costs, superior catalytic performance of noble metals in comparison with non-precious counterparts as well as established technologies for the recycling of the spent catalysts justify their application in different industrial catalytic processes ensuring overall profitable performance.

The aim of this work was to investigate kinetics in HDO of isoeugenol over bifunctional Pt- and Ir-modified H-Beta catalysts with different acidity and compare their performance with Pt- and Ir-supported on MCM-41, since mesoporosity can have beneficial effects in HDO of phenolic compounds. [18] Ir can also be beneficial in HDO, since it is known to exhibit hydrogenolysis activity. [28] In addition mildly acidic Pt/Al$_2$O$_3$ and non-acidic Ir/SiO$_2$ were also studied in order to elucidate the role of acidity, support structure and metal in HDO of eugenol. For the best Pt-H-Beta-300 catalyst, also catalyst reuse after regeneration and reduction was successfully demonstrated. Kinetics of (iso)eugenol hydrodeoxygenation has been scarcely investigated.[22, 25, 26] In the current work thermodynamic analyses for isoeugenol hydrodeoxygenation was performed using a thermodynamic approach [29] and the Gibbs-Helmholtz equation. The intention was to use the reaction network shown in Scheme 1, which was supported by the literature data, and to take into account reaction stoichiometry in the liquid phase. Furthermore, kinetic modelling of HDO of isougenol was also made in the current work. According to our knowledge kinetic modelling of HDO of eugenol has only been made in ref [22], where also mass transfer limitations and hydrogen solubility were considered.

Results and discussion

Catalyst characterization results

XRD results showed for Pt-H-Beta-300 and Ir-H-MCM-41 both X-ray powder diffraction patterns clearly showed that both Pt [32] and IrO$_2$ [33] were observed in the diffractograms in addition to Cu [34] in some cases originating from the sample holder due to a low amount of catalyst. Furthermore, X-ray powder diffraction patterns clearly showed that the structure of H-Beta-300 (Figure 1) remained intact after loading of Pt and the same is valid for Ir-HMCM-41 (Figure S1). [29-36]

Pt-H-Beta-300 catalyst exhibited the highest specific surface area (Table 1). The spent Pt-H-Beta-300 catalyst, after its use in hydrodeoxygenation of isoeugenol showed almost the same surface area (681 m^2/g) and the pore volume (0.24 cm^3/g). The reason for a minor decrease in the surface area for the spent Pt-H-Beta-30 catalyst as compared to the fresh Pt-H-Beta-300 catalyst can be attributed to coke deposition in the pores of the catalyst, although the pore volume remained constant. Pt-H-Beta-300 spent zeolite catalyst was regenerated in an oven using the step calcination procedure for 120 min. The regenerated Pt-H-Beta-300 catalyst exhibited the surface area of 650 m^2/g. The decrease in the surface area of the regenerated catalyst as compared to the spent could be due to the generation of mesoporous during the calcination procedure. However, it should be mentioned here that the obtained surface area and pore volume for the Pt-H-Beta-300 regenerated is higher than that of Pt-H-Beta-150 (621 m^2/g) and Pt-H-Beta-25 (592 m^2/g) fresh catalysts (Table 1).

The Pt-H-MCM-41 catalyst also exhibited a high specific surface area (679 m^2/g) and a large pore volume (0.45 m^2/g) (Table 1). The specific surface areas of Pt- and Ir-supported on silica and alumina were the lowest ones for all studied catalysts.

The results from the acidity measurements of Pt- and Ir-modified zeolites and mesoporous materials are shown in Table 2. The amount of Brønsted acid sites measured for pyridine desorbed at 250 °C indicates the sum of weak, medium and strong acidic sites. The highest amount of Brønsted acid sites was observed in Pt-H-Beta-25, which was more than four fold that of Pt-H-Beta-150 and nearly 9 fold compared to Pt-H-Beta-300. These results are in line with Si/Al ratio. Mesoporous Pt-H-MCM-41 and Ir-H-MCM-41 exhibited mild acidity, which is expected from MCM-41 in comparison with zeolite beta. Noteworthy is that the Brønsted acidity of Ir-H-Beta-150 was 1.6 fold higher than that of Pt-H-Beta-150. These catalysts did not contain any strong Brønsted acid sites (Table 2).

5

The highest amount of Lewis acid sites was also measured for Pt-H-Beta-25. Interestingly the second and third highest amounts of Lewis acid sites were determined for Pt-H-MCM-41 and Ir-H-MCM-41.

The scanning electron microscopy was used to study the shape, size and distributions of the crystals of Pt- and Ir-modified catalysts (Figure 2, 3, S2, S3). The Pt-H-Beta-300 exhibited spherical shaped crystals with the size ranging from 200 – 600 nm and the spent particles resemble the fresh ones (Figure 2). The Pt-H-Beta-150 and Pt-H-Beta-25 exhibited smaller crystal sizes (Figure 3), than the Pt-H-Beta-300. It is important to mention that the Pt- and Ir-modified H-Beta-300, H-Beta-150 and H-Beta-25 zeolite catalysts maintained the crystal morphology after the modification with hexachloroplatinic and iridium chloride solutions.

The Pt-H-MCM-41 mesoporous catalysts showed similar crystal morphology (Figure S2a) as the pristine H-MCM-41 (not shown here), indicating that the modifications of the mesoporous support using hexacloroplatinic acid and iridium chloride did not change the basic structure. The size of Ir-H-MCM-41 was ranging from 100 nm to 1000 nm (Figure S2b).

Pt-, Ir- particle size, structures of pores and periodicity of the pores for Pt-H-Beta-25, Pt-H-Beta-150, Pt-H-Beta-300, Ir-H-Beta-150, Pt-H-MCM-41 and Ir-H-MCM-41 catalysts, both fresh and used in hydrodeoxygenation of isoeugenol, at 200 ^{0}C and 3 MPa, were also characterized by transmission electron microscopy. TEM images revealed that the fresh and spent Pt- and Ir-modified catalysts exhibited similar structures to that of pristine Beta and MCM-41 catalysts (Figures 4-6, S4-5). The modifications of the microporous Beta zeolite and mesoporous MCM-41 with hexachloroplatinic acid and iridium chloride did not influence the parent structures of the supports. Similar observations were obtained in characterization of Pt-, Ir- modified Beta and MCM-41 mesoporous catalysts using X-ray powder diffraction. Pt particles were spherical, square and triangular, with the majority of them being spherical.

6

Pt-particle size of Pt-H-Beta-300 fresh calculated from the histograms was in the range 5-35 nm (Figure 4). The same catalyst after use in hydrodeoxygenation of isoeugenol exhibited the Pt- particle size in the range 5-40 nm, which is a sign of minor sintering. An average Pt- particle size calculated from the histogram was 11.1 nm.

Pt-H-Beta-300 spent catalyst was regenerated in an oven for 120 min followed by its reuse in hydrodeoxygenation of isoeugenol. Pt-particle sizes were in the range of 5-35 nm (Figure 4e and f), close to that of fresh Pt-H-Beta-300, clearly indicating that the spent catalyst after hydrodeoxygenation of isoeugenol can be regenerated and that the Pt-particle size was only slightly increased. In addition, the regenerated Pt-H-Beta-300 exhibited similar activity as the fresh one as explained below.

The particle size distributions of Pt-H-Beta-150 is given in the histogram of Figure 5. It is significant to mention that the Pt-particle size distribution of this catalyst was 5-10 nm for the fresh and spent catalysts, which is much lower than that of Pt-H-Beta-300. The latter was in the range of 5-35 nm. The plausible explanation for lower Pt-particle size distributions in Pt-H-Beta-150 catalyst is attributed to a smaller size of Beta-150 (50 -300 nm). The average Pt-particle size of Pt-H-Beta-150 was 6.2 nm (Figure 5).

The fresh and spent Pt-H-Beta-25 catalysts exhibited the Pt- particle sizes between 3-6 nm (Figure 6), with the average Pt-particle size of 3.4 nm. This catalyst showed the smallest average Pt- particle size of the three Beta catalysts studied. The average Pt- particle sizes for the fresh Pt- modified Beta zeolite catalyst were Pt-H-Beta-300 (11.1 nm) > Pt-H-Beta-150 (6.2 nm) > Pt-H-Beta-25 (3.6 nm). From these results, it can be concluded that the crystal size of Beta zeolite and acidity (Brønsted and Lewis) influenced the Pt-particle size. The largest crystal size and the lowest amount of Brønsted acid sites (Table 2) in Beta-300 resulted in the largest average Pt- particle size (11.1 nm). Analogously the high density of the surface hydroxyl

groups and interaction of metal- metal-oxide supports have been suggested as the reason for the decreased Rh particle size in Rh/Al$_2$O$_3$/SiO$_2$ compared to Rh/SiO$_2$ with the Rh particle sizes being 1.2 nm and 2.7 nm, respectively. [37]

The metal dispersion determined by CO pulse chemisorption is shown in Table 1. The highest metal dispersion was obtained in Pt/Al$_2$O$_3$ followed by Pt-H-Beta-25, whereas the lowest dispersions were determined for Ir/SiO$_2$ and Ir-H-Beta-150. The Pt particle sizes correlated well with TEM data for Pt-H-Beta-150 and Pt-H-Beta-300, except Pt-H-Beta-25 displaying a higher value according to CO chemisorption (Table 1).

The thermogravimetric analysis of the fresh and spent catalysts (Figure 7) was performed to determine the amount of coke present in the spent catalysts after hydrodeoxygenation of isoeugenol. Characterization of coke by TGA analysis (Figure 7) showed 3.6 wt% weight loss from the spent Pt-H-Beta-300 catalyst in the temperature range of 100 -1000 °C after utilization of this catalyst in isoeugenol HDO at 200°C under 3 MPa. The weight loss for the fresh catalyst was 1.9 wt% indicating that 1.7 wt% of organic material was adsorbed on the catalyst surface. The corresponding weight losses for the fresh and spent Pt-H-Beta-25 were 6% and 11.5 %, respectively, indicating that 5.5 wt% organic material was accumulated on a more acidic catalyst.

Thermodynamic analysis of isoeugenol hydrodeoxygenation

Enthalpy (ΔH^0_r) and Gibbs free energy (ΔG^0_r) at standard conditions were calculated using a thermodynamic approach, [29] starting from the standard enthalpy (ΔH^0_f) and Gibbs free energy (ΔG^0_f) of formation from the elements derived from the database included in ChemCAD v.5.0 [37] or estimated with the Joback approach, [39]

$$\Delta H^0_{r,j} = \sum_j v_{i,j} \cdot \Delta H^0_{f,i}$$

(1)

8

$$\Delta G^0_{r,j} = \sum_j \nu_{i,j} \cdot \Delta G^0_{f,i}$$

(2)

The equilibrium constant of each reaction was calculated from

$$K^0_j = exp\left(-\frac{\Delta G^0_{r,j}}{RT}\right)$$ (3)

The dependency of the reaction free Gibbs energy with temperature was included by

implementing the Gibbs-Helmholtz equation valid at P=0.1 MPa ($\Delta G^{\Phi}_{r,j}$):

$$\frac{\Delta G^\phi_{r,j}(T)}{T} = \frac{\Delta G^0_{r,j}}{T^0} + \Delta H^0_{r,j}\left(\frac{1}{T} - \frac{1}{T^0}\right)$$ (4)

Finally, to calculate the $\Delta G_{r,j}$ at different pressures Eq. (5) was implemented.

$$\Delta G_{r,j}(P) = \Delta G^\phi_{r,j} + nRT \ln\left(\frac{P}{P^0}\right)$$ (5)

in which n is moles. In thermodynamic modelling the reactions shown in Table 3 and

Scheme 1 were modelled. The stoichiometry used in Table 3 was applied. The calculated

enthalpy and Gibbs free energy formation for each component (*i*) are reported in Table S1. The

data were retrieved from ChemCAD v.5.0 database directly.

Starting from these values, the enthalpy and Gibbs free energy for each reaction (*j*) at

standard conditions, equilibrium constants at standard conditions *(K^0_j)*, enthalpy and Gibbs free

energy at different temperatures and pressure were calculated. Two different temperatures were

investigated (T_1=473.15 K, T_2=573.15 K) and the energy values were calculated also at P_1=3

MPa.

Thermodynamic analyses shows that thermodynamically not feasible reactions for

propylcyclohexane are the steps 5, 6 and 9 (Table S2) corresponding to de-ethylation and

alkylation of propylcyclohexane forming 1-methyl-3-ethylhexane, isomerization forming

isopropylcyclohexane and its ring contraction forming 1-methyl-3-propylcyclopentane. In

9

addition, hydrogenation of the intermediate propylbenzene became unfeasible at a higher temperature, 300°C compared to 200°C (step 4). Higher pressure favored demethoxylation of dihydroeugenol and formation of methanol (step 2).

Catalytic results from the transformation of isoeugenol with Pt- and Ir- modified catalysts

Isoeugenol transformations over Pt- and Ir-modified beta zeolite catalysts

Isoeugenol transformation was investigated with Pt supported on alumina, silica, H-MCM-41 and Beta zeolites with three different SiO_2 to Al_2O_3 ratios (Table 4). The transformation of isoeugenol is very rapid with Pt-Beta zeolite catalysts and thus TOF values were calculated for the transformations of its hydrogenated product - dihydroeugenol within the first 30 min. Interestingly the most active catalyst in hydrodeoxygenation was Pt-H-Beta-300 (Figure 11, Table 4, entry 1) exhibiting the lowest Brønsted acidity from the studied Pt-H-Beta catalysts (Table 2). The second most active catalyst was Pt-H-Beta-150, whereas TOF for the most acidic catalyst Pt-H-Beta-25 was only 47% of that of Pt-H-Beta-150. These results indicate that too high amount of acid sites is not beneficial for dihydroeugenol transformation. Since the metal particle sizes vary only slightly in these three Pt-H-Beta zeolite catalysts, it was also decided to perform experiments with Pt-H-Beta-25 calcined at higher temperatures in order to increase the Pt particle size (see below).

Isoeugenol was hydrogenated very rapidly to dihydroeugenol and thus conversion of dihydroeugenol was compared (Table 4, Figure 8) over three Pt-H-Beta catalysts with different acidity. All these catalysts were active during the whole reaction time and high conversions were obtained (Table 4, entries 1-3). The sums of the liquid phase masses of the reactant and products determined by GC were calculated from the liquid phase. A trend of this sum decrease with an increase of the amount of Brønsted acid sites follows from Figure 9. In fact, this sum

10

should be ca. 77%, if all dihydroeugenol is deoxygenated and demethoxylated to propylcyclohexane and the formation of water and methanol is not taken into account. The sum of the liquid phase masses of the reactant and products determined by GC (Table 4) for Pt-H-Beta-150 and Pt-H-Beta-25 was lower than the theoretical mass balance. Furthermore, the sums of liquid phase masses of the reactant and products determined by GC without hydrodeoxygenation were ca. 100% when only hydrogenation occurred (Figure 9). Incomplete liquid phase mass balance determined by GC can be in general explained by oligomerisation of some products, as well as strong adsorption of organic compounds on the catalyst surface and formation of gas phase products. Oligomers, however, could not be detected by GC analysis. When considering GC results and by taking into account the accumulated organic material on the catalyst surface, a slightly higher sum of liquid phase reactant and products determined by GC was recorded for Pt-H-Beta-300 and Pt-H-Beta-25 (Table 4). Analogous of the data in the current work and comparison with literature allows to conclude that for isoeugenol HDO at 170°C under 4 MPa hydrogen in water as a solvent over acidic catalysts, such as Ru/ZSM-5 [21] a too high value of the sum of liquid phase masses of the reactant and products determined by GC was reported (91.4%) as the main product was propylcyclohexane. Analogously the overall product yields was reported to be 99.5% for isoeugenol HDO over Co/H-ZSM-5 under 1 MPa hydrogen in dodecane as a solvent at 200°C although 87% of the products were demethoxylated ones indicating that there might be some inconsistencies in the calculations of the sum of the liquid phase masses for the reactant and products determined by GC. [25] In deoxygenation of isoeugenol over Raney nickel (H-ZSM-5) at 220°C under nitrogen in a methanol- water mixture the sum of calculated products was 96.4% at 97.2 % conversion. In addition, 89.1% of demethoxylated products were formed, [20] which is too high if methanol was not taken into account. Furthermore, the propylcyclohexane yield of 100% was reported in ref. [26] in HDO of eugenol at 200°C under 2 MPa hydrogen over CoNx catalyst. These examples show that

11

quantitative analysis of the reaction mixture is challenging and that the data reported in the literature should be critically evaluated.

For comparison of Pt- and Ir-catalysts, also Ir-Beta-150 was tested in isoeugenol hydrodeoxygenation (Table 4, entry 4). This catalyst despite being more acidic than Pt-H-Beta-150 exhibited a low TOF towards dihydroeugenol transformation, most probably due to its large Ir-particle size. This comparison clearly shows that the metal dispersion has a significant role in HDO in line with the literature. [23] Because of Ir-H-Beta-150 acidity (Table 2) also some heavy products, such as dimeric isoeugenol and 2,2'-methylene-bis(1,1-dimethylethyl)-4-methylphenol were observed by GC-MS (Figures S6, S7). It should be pointed out here, that these compounds did not elute from the same GC column in quantitative GC analysis in this study. Since Ir can promote according to the literature hydrogenolysis, [28] it was decided to explore catalytic activity of highly dispersed iridium supported on non-acidic silica in deoxygenation of dihydroeugenol.

The effect of the metal particle size in hydrodeoxygenation of isoeugenol was also investigated using Pt-H-Beta-25 calcined at 650° C and 850 °C (Table 4, entry 5 and 6). As expected, high temperature treatment was detrimental for catalytic activity and Pt-H-Beta-25 (850°C) exhibited a very low reaction rate compared to Pt-H-Beta-25 calcined at either 450°C or 650°C, which can be explained by low acidity and a larger metal particle size (Tables 1, 2). It is also interesting to note that the sum of liquid phase masses of the reactant and products determined by GC was much lower for a more acidic Pt-H-Beta-25 (650°C), which exhibited a large number of acid sites. At the same time this sum for Pt-H-Beta-25 (850°C) was 87%, as the latter catalyst is only mildly acidic due to dealumination occurring for beta zeolite at higher temperature breaking also the twelve member ring. [40] Such behavior can in part explain low acidity of Pt-H-Beta-25 (850° C) (Table 2).

12

The degree of hydrodeoxygenation with three Pt-H-Beta zeolites was 100% showing that bifunctional catalysts are required for this reaction. The main product and its selectivity after 4 h are shown for all catalysts in Table 4. Propylcyclohexane was the main product for Pt-H-Beta-300, Pt-H-Beta-150, Pt-H-Beta-25 (Figure 8c) and the selectivity towards propylcyclohexane increased also with decreasing the catalyst acidity (Table 4, entries 1-3, Figure 8c). Dialkylated cyclohexanes were also formed as minor products using Pt-beta zeolites as catalysts (Table 4). The GC-MS identification showed that most probably the main side products over Pt-H-Beta-25 were isomers of 1-ethyl-2-methyl-cyclohexane (Figure S8). The mass spectrum of exactly this molecule was not found in the mass spectra library, however, data for two other isomers, namely *trans*-1-ethyl-4-methylcyclohexane and *cis*-1-ethyl-2-methylcyclohexane are available in the NIST library. When comparing the MS of the product formed over Pt-H-Beta-25, it can be clearly seen that it has the cleavage fragments with m/z at 111 and 97 corresponding to cleavage of methyl and ethyl groups. Furthermore, these fragments are not found in propylcyclohexane fragments. It can be thus concluded that two main side products over Pt-H-Beta-25 are dialkylated cyclohexanes containing nine carbon atoms. Formation of these products includes breaking of the C-C bond in the propyl chain and alkylation of the phenyl ring, whereas only alkylation is needed for formation of 1-methyl-4-ethylcyclohexane. It should, however, be noted that 1-methyl-3-propylpentane exhibiting the molecular mass of 126 g/mol, i.e. the same as for propylcyclohexane, was stated to be a product in eugenol HDO over Ru/C.[22] Traces of propylbenzene were also formed over Pt-H-Beta-25, indicating a slightly lower ring hydrogenation activity after prolonged reaction times. In addition over this catalyst also 1-methyl-2-propylcyclopentane was formed in small amounts by ring contraction of propylcyclohexane. Activity of Pt in ring contraction has been reported previously. [13] The main product over Ru/H-ZSM-5 in isoeugenol HDO in water at 170°C under 4 MPa hydrogen was propylphenol.[21] Both propylcyclohexanol and 1-methyl-3-

13

ethylcyclohexane were formed in HDO of eugenol at 200°C under 0.5 MPa hydrogen over Raney nickel catalyst supported on H-ZSM-5 [20] analogously to the current results. Noteworthy is also that propylcyclohexanol and propylphenol were the main products in HDO of eugenol over Co-H-ZSM-5 at 200°C under 1 MPa hydrogen and no propylcyclohexane was formed despite of the reported acidity of Co-H-ZSM-5. [25] Kinetics of isoeugenol HDO over Pt-H-Beta-300 and Pt-H-Beta-25 is shown in Figure 10 and will be discussed below.

Experiment with Pt-H-Beta-25 calcined either at 650°C or 850 °C showed the further transformations of isoeugenol were slow and the main product was dihydroeugenol (Figure 11). When comparing the current results with the data in [22] when HDO of eugenol was performed over Ru/C at 270°C in hexadecane as a solvent, it can be noticed that the main products in ref. [22] were dihydroeugenol and propylphenol in line with the current results. Zeolites are more acidic than Ru/C and thus more propylcyclohexane is formed in the current work.

Isoeugenol transformation over Pt- and Ir-modified MCM-41 catalysts

Isoeugenol was hydrogenated rapidly to dihydroeugenol over Pt-H-MCM-41 and Ir-H-MCM-41 despite large metal particle sizes (Figure S9). Further transformations of dihydroeugenol were very slow over Ir-H-MCM-41, whereas over Pt-H-MCM-41 the selectivity of propylcyclohexane was 35% already after 4 h (Table 4, entry 7). Noteworthy is also that over Pt-H-MCM-41 with mesopores the selectivity of propylcyclohexane was 1.9 fold higher than with microporous Pt-H-Beta-25 (650 °C) exhibiting four fold higher Brønsted acidity. This result indicates that mesoporosity is beneficial for hydrodeoxygenation of isoeugenol facilitating easier product diffusion from the pores to the bulk liquid. This result correlates with the kinetic diameter of eugenol equal to 8.97 Å calculated using Chemsketch [18] which is larger than the cavities of beta zeolite exhibiting channels with a cross section of 6.6 Å * 6.7 Å and a sinusoidal channel with a cross section of 5.6 Å * 5.6 Å. [42] The pores of

14

MCM-41 are typically quite large, for example for Al-MCM-41 with Si/Al ratio of 5 the pores with the size of 3.3 nm were found. [41] Zhang et al. [18] also confirmed that mesoporosity is beneficial for eugenol hydrogenation.

Isoeugenol transformations over Pt- and Ir-catalysts supported on silica and alumina

Isoeugenol hydrodeoxygenation was investigated in this work using Pt/Al$_2$O$_3$ bearing Lewis acidity as well as very mildly acidic Pt/SiO$_2$ and Ir/SiO$_2$ catalysts (Table 4, entries 7-9). Hydrogenation of isoeugenol per se proceeded rapidly over these catalysts showing also that further reactions of dihydroeugenol were, as expected, of minor importance due to the non-acidic character of the catalysts. The main product was thus always dihydroeugenol with a very high selectivity.

Main parameters affecting hydrodeoxygenation selectivity

Effect of the amount of Brønsted acid sites on selectivity to the main product, propylcyclohexane after 4 h reaction time in hydrodeoxygenation of isoeugenol is summarized in Figure 12 showing clearly that a high amount of Brønsted acid sites is not the only parameter influencing selectivity to propylcyclohexane. One example is a relatively high acidity of Pt-H-Beta-25 calcined at 650°C, which afforded only 18% selectivity towards propylcyclohexane. For this catalyst a lower HDO activity is explained by a large Pt particle size not favoring even HDO of the formed dihydroeugenol (Table 4, entry 5).

Reuse of Pt-H-Beta-300

Reuse of the calcined Pt-H-Beta-300 catalyst in dehydrodeoxygenation of isoeugenol (Figure 13) shows clearly that it is possible to recover the catalytic activity of this catalyst nearly completely even if the pore volume of the regenerated catalyst was only 78% of the fresh one.

Kinetic modelling

Kinetic modelling of isoeugenol hydrodeoxygenation was performed for three Pt-H-Beta catalysts with different acidities using pseudo first order simplified kinetic equations. The reaction scheme is shown in Figure 14. The intermediate C has only been confirmed in the case of Pt-H-beta-300 exhibiting the mildest acidity, whereas with more acidic catalysts its further reaction is so rapid, that it has not been identified in the reaction products

Rate equations for Pt-H-Beta-300 have been defined as:

$$r_1 = k_1 c_A \tag{6}$$

$$r_2 = k_2 c_B \tag{7}$$

$$r_3 = k_3 c_C \tag{8}$$

$$r_4 = k_4 c_D \tag{9}$$

$$r_5 = k_5 c_A \tag{10}$$

$$r_7 = k_7 c_B \tag{11}$$

where k_i correspond to the rate constants of the steps from Figure 14. The concentrations of products p_1, p_2 p_3 and p_4 have been lumped, due to their small amounts. Their generation is described by r_7.

The corresponding mass balances for the batch reactor are:

$$\frac{dc_A}{dt} = -r_1 - r_5 - r_6 \tag{12}$$

$$\frac{dc_B}{dt} = r_1 - r_2 - r_6 \tag{13}$$

$$\frac{dc_C}{dt} = r_2 - r_3 + r_4 - r_8 \tag{14}$$

$$\frac{dc_D}{dt} = -r_3 - r_4 - r_9 \tag{15}$$

$$\frac{dc_E}{dt} = r_5 \tag{16}$$

$$\frac{dc_F}{dt} = r_6 + r_7 + r_8 + r_9 \tag{17}$$

16

For more acidic catalysts, i.e. Pt-H-Beta-25 and Pt-H-Beta-150 more simplified rate equations have been used:

$$r_1 = k_1 c_A \tag{18}$$

$$r'_2 = k'_2 c_B \tag{19}$$

$$r_5 = k'_5 c_A \tag{20}$$

$$r'_7 = k'_7 c_B \tag{21}$$

The differential equations were solved with the backward difference method as a subtask to the parameter estimation with simplex and Levenberg-Marquardt methods. The numerical tools are built into the used software Modest, [43] in which the objective function was defined as

$$\theta = \sum (y_i - \hat{y}_i)^2 \tag{22}$$

and the degree of explanation R^2 is defined as

$$R^2 = 1 - \frac{\sum (y_i - \hat{y}_i)^2}{\sum (y_i - \bar{y}_i)^2} \tag{23}$$

in which $\bar{y}_i$ is the mean value of observations. The parameters for different catalysts are shown in Table 5 and the corresponding data fitting results are given in Figure 10. Overall the parameters were well defined, apart from k_5' for Pt-H-Beta-25, for which quite high correlation with k_1 and k'_2 was observed (Table S3). The degree of explanation was for Pt-H-Beta-300 98.36%, whereas it was for Pt-H-Beta-25 95.63%. It can be concluded that the proposed models could describe the kinetic data well.

In addition to the model presented in Fig. 14, an alternative model shown in Scheme 1 was tested. This model implies first demethoxylation of dihydroeugenol followed by hydrogenation of the phenyl ring in 4-propylphenol, because dehydration of OH-group from the aromatic ring might be less probable. Thereafter, dehydroxylation of 4-propylcyclohexanol should proceed rapidly and it is possible that propylbenzene is formed in the presence of hydrogen even at 200°C via dehydrogenation of propylcyclohexane. The thermodynamics of

17

this reaction is not favorable as the logarithm of the equilibrium constant of a gas phase hydrogenation reaction (i.e. reverse to dehydrogenation) at 200°C is ca. 4. Nevertheless, kinetic modelling cannot discriminate between these two models as the results using the alternative model gave an also an adequate description.

18

Conclusions

Pt- and Ir-modified H-Beta-25, H-Beta-150 and H-Beta-300 microporous zeolites, structured MCM-41 with mesopores and SiO_2 were synthesized by an evaporation impregnation method. Pt-H-Beta-300 catalyst with the smallest amount of Brønsted acid sites exhibited with the largest crystal size and Pt size.

The highest conversion in hydrodeoxygenation of isoeugenol and selectivity to the desired cycloalkanes were obtained over Pt-H-Beta-300 catalyst. The highest amount of Brønsted acid sites was present in Pt-H-Beta-25 followed by Pt-H-Beta-150, Pt-H-MCM-41 and Pt-H-Beta-300.

With the best catalyst the selectivity to propylcyclohexane was 89% at complete conversion of isoeugenol. When more acidic Pt-H-Beta zeolites were applied, the selectivity towards propylcyclohexane decreased at the same time increasing the amount of dialkylated cyclohexanes indicating cleavage of propyl group and alkylation of the cyclohexane. The sum of the liquid phase masses of the reactant and products determined by GC decreased with increasing catalyst acidity due to formation of oligomers as well as formation of gaseous products and accumulation of organic material on the catalyst surface.

Pt-H-Beta-25 calcined at 650°C with lower metal dispersion, but still exhibiting high acidity, was giving dihydroeugenol as the main product. This result indicates that high metal dispersion and certain acidity are required for efficient isoeugenol hydrodeoxygenation. The same conclusion can be drawn from the data for a non-acidic Ir/SiO_2 catalyst exhibiting rather small Ir particles. This catalyst did not lead to efficient deoxygenation of isoeugenol, even if iridium is known to catalyze hydrogenolysis.

The spent best catalyst, Pt-H-Beta-300 used for hydrodeoxygenation of isoeugenol could be regenerated regaining the catalytic properties. The regenerated Pt-H-Beta-300 catalyst

19

exhibited almost the same conversion of isoeugenol and selectivity to cyclohexane as the fresh Pt-H-Beta-300, indicating catalyst reusability.

Pt-H-MCM-41 catalyst with large mesopores (4.9 nm) exhibited almost twofold higher selectivity to propylcyclohexane than microporous Pt-H-Beta-25 (650 °C) with pores of 0.7 nm size and four fold larger amount of Brønsted acid sites. It was found that the particle size of Pt and Ir, appropriate amounts and strength of Brønsted and presumably Lewis acid sites, pore size and structure of the catalysts are of importance for hydrodeoxygenation of isoeugenol.

Experimental

Catalyst preparation

Three Pt-modified Beta zeolite catalysts with SiO_2 to Al_2O_3 ratios of 25, 150 and 300 were prepared from NH_4-Beta (Zeolyst International) as starting materials. The support materials were calcined at 450°C to obtain the proton form. Pt- and Ir-modified H-Beta-300, H-Beta-150, H-Beta-25 microporous zeolites, H-MCM-41 structured material with mesopores and SiO_2, supported catalysts were synthesized using an evaporation impregnation method in a rotavapor equipment. Aqueous solutions of hexachloroplatinic acid (Merck) and iridium chloride (Merck) were used as Pt- and Ir-metal precursors. Ir/SiO_2 was prepared with the same method by addition of iridium to silica gel (Merck) using chloropenta amine iridium(III) chloride (Alfa Aesar) as an iridium source. The duration of catalyst synthesis was 24 h, after which the catalysts were removed from the flask and dried in an oven. The thermal treatment of the Pt- and Ir-modified catalysts was carried out in a muffle oven using the step-calcination procedure (Table S4). The calcined catalysts were weighed and stored in sealed bottles.

MCM-41 structured mesoporous material was synthesized using the method described in ref [44]. The silica to alumina ratio of Pt-H-MCM-41 structured mesoporous catalyst was 20.

Catalyst characterization methods

X-ray powder diffraction

The Philips X'Pert Pro MPD X-ray powder diffractometer was used for the characterization of the structure and phase purity of Pt- and Ir- modified microporous zeolites and mesoporous catalysts. The diffractometer was operated in Bragg-Brentano diffraction mode, and the monochromatized Cu-$K\alpha$ radiation ($\lambda = 1.541874$ Å) was generated with a voltage of 40 kV and a current of 45 mA. The primary X-ray beam was collimated with a fixed 0.25° divergence slit and a fixed 10 mm mask. A 7.5 mm anti-scatter slit was used in the diffracted beam side prior to the proportional counter.

For all the samples, the measured 2θ angle range was 5.0°−85.0°, with a step size of 0.026° and measurement time of 10 s per step. For Ir-H-MCM-41 and 2 wt% Pt-H-MCM-41, the diffractograms were also determined with smaller 2θ angles in order to observe the diffraction peaks originating from the MCM-41 phase. In these measurements, the applied 2θ angle range was 0.8°−9.8°, with a step size of 0.02° and measurement time of 10 s per step. A 0.18° parallel plate collimator was used in the diffracted beam side prior to the proportional counter. The samples were placed on copper sample holders. The phase detection threshold was ca. 5 %.

The diffractograms were analyzed with Philips X'Pert HighScore and MAUD (http://www.ing.unitn.it/~maud/) programs. HighScore together with MAUD was used for the phase analysis and MAUD for the Rietveld refinement. The Powder Diffraction File 2 (PDF-2) database, IZA Structure Commission Database of Zeolite Structures and Inorganic Crystal Structure Database (ICSD) were used as in refs [36, 45-47]. The crystal structure reference and the corresponding crystal information (.cif) file of Beta polymorph A (SiO$_2$ framework) were taken from the IZA Structure Commission Database of Zeolite Structures. [46]

21

Transmission electron microscopy

Transmission electron microscopy was used to determine the size of Pt- and Ir-metal particles for the fresh and spent catalysts. TEM was also used to study the porous structure and periodicity of pores of the catalysts. The instrument used for the measurements was JEM 1400 plus with an acceleration voltage of 120 kV and with resolution of 0.98 nm using Quemsa II MPix bottom mounted digital camera.

Scanning electron microscopy (SEM) and Energy dispersive X-ray micro-analyses (EDXA)

Morphology of Pt- and Ir-catalysts for namely the crystal shape, size and distributions were investigated with scanning electron microscopy (SEM), Zeiss Leo Gemini 1530 microscope equipped with SE (secondary electron) and BSE (backscattered electron) devices. The chemical compositions of some selected fresh and spent catalysts was investigated using energy dispersive X-ray-microanalyses (EDXA).

Nitrogen adsorption

The specific surface area, pore volume and pore size distributions of the catalysts were determined using nitrogen adsorption method with Sorptomatic 1900 (Carlo Erba Instruments). The sample was outgassed prior to the experiment at 150°C for 3 h. Specific surface area and the micro-pore volume for the microporous zeolites were calculated with Dubinin and Horvath/Kawasaki methods, respectively. [45] The specific surface and the pore volume of the mesoporous catalysts were calculated using BET and Dollimore /Hill methods, respectively.

CO pulse chemisorption

The metal dispersion and particle sizes were determined with CO pulse chemisorption using Autochem 2910. Prior to measurements about 100 mg of catalyst was prereduced with the

22

following temperature programme: 10°C/min- 450 °C (3 h). Thereafter, the catalyst was flushed at 350 °C for 90 min with argon in order to remove adsorbed hydrogen. Then the catalyst was cooled to room temperature. CO was adsorbed for 40 min min using 10 vol % CO in helium (AGA). Thereafter chemisorbed CO was removed by flushing the catalyst with helium. The pulse chemisorption measurement was performed at 25 °C and the stoichiometry 1:1 for Pt:CO [48] and 1:1.19 Ir:CO [49] was applied for calculating the metal particle size.

Measurement of the acid sites using FTIR-pyridine adsorption desorption

Characterization of the Brønsted and Lewis acid sites, their amount and strength was determined using pyridine (Sigma Aldrich, ≥ 99.5 % a.r.) adsorption-desorption. The measurements were performed with ATI Mattson FTIR using 10 mg of self –supported catalyst pellets. In order to discriminate between weak, medium and strong acid sites, desorption of pyridine was performed at 250°C, 350°C and 450 °C, respecitvely. Quantification of Brønsted and Lewis acid sites was done by considering intensity of IR signals at 1545 cm^{-1} and 1455 cm^{-1}, respectively, using the molar extinction factor given by Emeis. [50]

Thermogravimetrical analysis

Thermogravimetric analysis of the fresh and spent catalysts was performed to analyze the amount of coke contents in the spent catalysts after use in hydrodeoxygenation of isoeugenol. The equipment used for the quantitative analysis of the coke contents was a Pyris-TGA, Perkin Elmer instrument under nitrogen flow of 20 ml/min to avoid oxidation of the sample. The amount of catalyst was ca. 7 mg. The mass loss was detected as a function of the temperature increase using the following temperature programme: 25 °C – 10°C/min – 1000°C under inert atmosphere.

Experimental setup for hydrodeoxygenation of isoeugenol

23

Isoeugenol transformation was typically performed in an autoclave using 100 mg of isoeugenol, 50 ml of dodecane (Sigma Aldrich, ≥99%). as a solvent and 50 mg preduced catalyst. All catalysts were reduced, firstly, started with Ar flushing for ten minutes and followed with H_2 flushing (10 min). The temperature programme for reduction was 350°C for 3 h with ramping of 10℃/min. Thereafter, hydrogen was replaced with argon and 10 ml of the solvent was added into the reactor containing the pre-reduced catalyst. The experiment was performed by placing the prereduced catalyst into the autoclave and additionally 40 ml of dodecane. The reactor was first flushed for 10 min with argon (AGA, 99.999%) and then by hydrogen (AGA, 99.999%). Thereafter the reactor outlet was closed and the reactor was pressurized at room temperature up to 2 MPa. Then the temperature was elevated to the desired temperature and finally the pressure was adjusted to 3 MPa. The reaction was started by turning on the stirrer and using 900 rpm in order to suppress the external mass transfer limitations. In order to make the experiments in the kinetic regime, small catalyst particles (below 63 µm) were used. The samples were periodically withdrawn to study the reaction kinetics. The spent catalyst was regenerated at 400°C for 160 min in the presence of air and thereafter reused.

The reuse of the most promising catalyst, Pt-H-Beta-300, was investigated using the regenerated and reduced catalyst in the second experiment with the same initial isoeugenol concentration as used in the first experiment. Pt-H-Beta-300 spent catalyst was regenerated in a muffle oven using step calcination procedure, specifically utilized for Pt containing catalysts (Table S1).

Analysis of the reaction mixture

The reaction mixture was analyzed by gas chromatography using DB-1 capillary column (Agilent 122-13e, 30 m internal diameter 250 µm, film thickness 0.50 µm) and a FID detector. The following temperature programme was used: 60°C (5 min) -3°C/min -300°C. The reaction

24

products were identified by GC-MS and quantified by making a calibration curve for the
following compounds: isoeugenol (Fluka, ≥98%), 4-propylcyclohexane (Aldrich, 99%),
dihydroeugenol (2-methoxy-4-propylphenol; Sigma Aldrich, ≥ 99%).

List of symbols

K^0_j	Equilibrium constant at standard conditions for reaction j
n	Moles, mol
P	Pressure, MPa
P^0	Standard pressure, MPa
R	Ideal gas constant, J/K/mol
R^2	Degree of explanation
T	Absolute temperature, K
T^0	Absolute standard temperature, K

Greek symbols

ΔG^0_f	Gibbs free energy of formation at standard conditions, J/mol
ΔG^0_r	Gibbs free energy of reaction at standard conditions, J/mol
$\Delta G^\Phi_{r,j}$	Gibbs free energy of reaction at 0.1 MPa and a chosen temperature, J/mol
$\Delta G_{r,j}$	Gibbs free energy of reaction at a fixed temperature and pressure, J/mol
ΔH^0_f	Enthalpy of formation at standard conditions, J/mol
ΔH^0_r	Enthalpy of reaction at standard conditions, J/mol
$v_{i,j}$	Stoichiometric matrix composed by i components and j reactions, -

References

[1] M. B. Polk, M. Phingbodhipakkiya, *Waste Management* **1980**, *1*, 111-118.

[2] S. Oh, G. H. Hwan, H. S. Choi, J. W. Choi, *Chemosphere*,**2014**, *117*, 806-814.

[3] A. V. Bridgewater, A. V., *Biomass Bioenergy* **2012**, *30*, 68-94.

[4] D. E. Kim, X. Pan, *Ind. Eng. Chem.* **2010**, *49*, 12156-12163.

[5] A. Jongerius, R. Gosselink, J. Dijkstra, J., Bitter, P. Bruijnincx, B. Weckhuysen, *ChemCatChem* **2013,** *5*, 2964 – 2972.

[6] R. N. Olcese, J. Francois, M. M. Bettahar, D. Petitjean, A. Dufour, *Energy Fuels* **2013**, *27*, 975-984.

[7] C. Sepuldeva, K. Leiva, R. Garcia, L. R. Radovic, I. T. Ghampson, W. J. DeSisto, J.L. Garcia Fierro, N. Escalona, *Catal. Today* **2011**, *172*, 232-239.

[8] V. N. Bui, D. Laurenti, P. Afanasiev, C. Geantet, *Appl. Catal. B: Environ*. **2011**, *101*, 239-245.

[9] P. M. Mortensen, J.-D. Grunwaldt, P. A. Jensen, G. Knudsen, A. Degn Jensen, *Catal Sci. Technol.***2014**, 3672-3686.

[10] I. T. Ghampson, C. Sepuldeva, R. Garcia, J. L. G. Fierro, N. Escalona, *Catal. Sci. Technol*. **2016**, *6*, 4356-4369.

[11] E. Santillan-Jimenez, M. Perdu, R. Pace, T. Morgan, M. Crocker, *Catalysts* **2015**, *5*, 424-441

[12] J. E. Peters, J. R. Carpenter, D. C. Dayton, *Energy Fuels* **2015**, *29*, 909-916.

[13] D. Gao, Y. Xiao, A. Varma, *Ind. Eng. Chem. Res.* **2015**, *54*, 10638-10644.

[14] M. Shetty, K. Murugappan, W. H. Green, Y. Roman-Leshkov, *ASC Sust. Chem. Eng.* **2017**, *5* (6), 5293–5301.

[15] Q. Lu, C.-J. Chen, W. Luc, J. G. Chen, A. Bhan, F. Jiao, *ACS Catal*. **2016**, *6*, 3506-3514.

[16] R. Lodeng, C. Ranga, T. Rajkhowa, V. I. Alexiadis, H. Bjorkan, S. Chytil, I. H. Svenum, J. Walmsley, J.W. Thybaut, *Biomass Conv. Bioref.* DOI 10.1007/s13399-017-0252-z

[17] A. K. Deepa, P. L. Dhepe, *ChemPlusChem* **2014**, *79*, 1573-1583.

[18] C. Zhang, J. Xing, L,. Song, H. Xin, S. Lin, L. Xing, X. Li, *Catal. Today* **2014,** *234*, 145–152

[19] X. Zhang, Q. Zhang, T. Wang, T. Ma, Y. Yu, L. Chen, *Biores. Technol*. **2013**, *134*, 73-80.

[20] J. Feng, C.-Y. Hse, K. Tang, J. Jiang, *Appl. Catal. A. Gen.* **2017**, *542*, 163-173.

[21] L. Wang, J. Zhang, X. Yi, A. Zheng, F. Deng, C. Chen, Y. Ji, F. Liu, X. Meng, F.-S. Xiao, *ACS Catal.* **2015**, 5, 2727-2734.

[22] A. Bjelic, M. Grilc, B. Likozar, *Chem. Eng. J.* **2018**, *333*, 240-259.

[23] A. Dwiatmoko, L. Zhou, I. Kim, J.-W. Choi, D. J. Suh, *Catal. Today* **2016**, *65*, 192-198.

[24] J. Qi, S.-F. Tang, Y. Sun, C. Xu, X. Li, *Chemistry Select* **2017**, *2*, 7525-7529.

[25] X. Liu, W. Jia, G. Xu, Y. Zhang, Y. Fu, *ACS Sustainable Chemistry Engineering* **2017**, *5*, 8594-8601.

[26] X. Liu, L. Xu, G. Xu, W. Jia, Y. Ma, Y. Zhang, *ACS Catalysis* **2016**, *6*, 11, 7611-7620.

[27] M. Y. Chen, Y.-B. Huang, H. Pang, X.-X. Liu, Y. Fu, *Green Chem.* **2015**, *17*, 1710-1717.

[28] A. J. Pamphile-Adrian, P. P. Florez-Rodriguez, F. B. Passos, *J. Braz. Chem. Soc.* **2016**, *77*, 5, 956-966.

[29] M.W. Zemansky, M.M. Abbott, H.C. Van Ness. Basic engineering thermodynamics. McGraw-Hill 1975.

[30] J. M. Newsam, M.M.J. Treacy, W. T. Koetsier, C. B. de Gruyter, *Proc. R. Soc. Lond. A* **1988**, *420*, 375-405.

[31] D. Das, P. J. E. Harlick, A. Sayari, *Catal. Commun.* **2007**, *8*, 829–833.

[32] O. A. Anunziata, A. R. Beltramone, J. Cussa, *Catal. Today* **2008**, *133-135*, 891-896.

[33] T. Swanson, *Natl. Bur. Stand. (U.S.), Circ.* **1953**, *539*, I, 31. (Pt)

[34] *Natl. Bur. Stand. (U.S.) Monogr.* **1965**, *25*, 4, 19. (Ir)

[35] T. Swanson, *Natl. Bur. Stand. (U.S.), Circ.* **1953**, *539*, I, 15. (Cu)

[36] Database of Zeolite Structures, *http://www.iza-structure.org/databases/*, June 2012, IZA Structure Commission.

[37] N. Yang, S. F. Bent, *J. Catal.* **2017**, *351*, 49-58.

[38] ChemCAD v.5.0, Chemstations (http://www.chemstations.com/)

[39] B.E. Poling, J. M. Prausnitz, J.P. O'Connell. The properties of gases and liquids (5th ed.) 2004. McGraw-Hill: New York.

[40] G. J. Wang, Y. Wang, Y. Liu, Z. Liu, Y. J. Guo, G. Liu, Z. Yang, M. X. Xy, L. Wang, L., *Appl. Clay Sci.* **2009**, *44*, 1-2, 185-188.

[41] S.-B. Liu, J.Wang, *J. Cat.* **1991**, *132*, 2, 432-439.

[42] C. Baerlocher, W. M. Meir, O. H. Olson, Atlas of Zeolite Framework Types, 5th revised ed.; Elsevier Science: Amsterdam, The Netherlands, 2001.

[43] H. Haario, MODEST Users guide, Profmath Oy, Helsinki 2007.

[44] T. Kresge, M. E. Leonovitz, W. J. Roth, J. C. Vartuli, US Patent 509,868,4, 1992.

[45] Powder Diffraction File 2 (PDF-2), sets 1-46, 1996 release, International Centre for Diffraction Data (ICDD).

[46] Inorganic Crystal Structure Database (ICSD), version 2.1.0, *http://www.fiz-karlsruhe.de/icsd.html*, April 2012, Fiz Karlsruhe.

28

[47] R. Ghezini, S. Sassi, A. Benqueddach, *Microp. Mesop. Mat.* **2008**, *113*, 370-377.

[48] K. Shinichi, Y. Yoshiteru S. Atsushi, H. Tadashi, *Journal of Japan Petr. Inst.* **2005**, *48*, 3, 173－177.

[49] S. J. Tauster, S. C. Fung, R. L. Garten, *J. Am. Chem. Soc.* **1978**, *100*, 170-175.

[50] C. A. Emeis, *J. Catal.* **1993**, *141*, 2, 347-354.

29
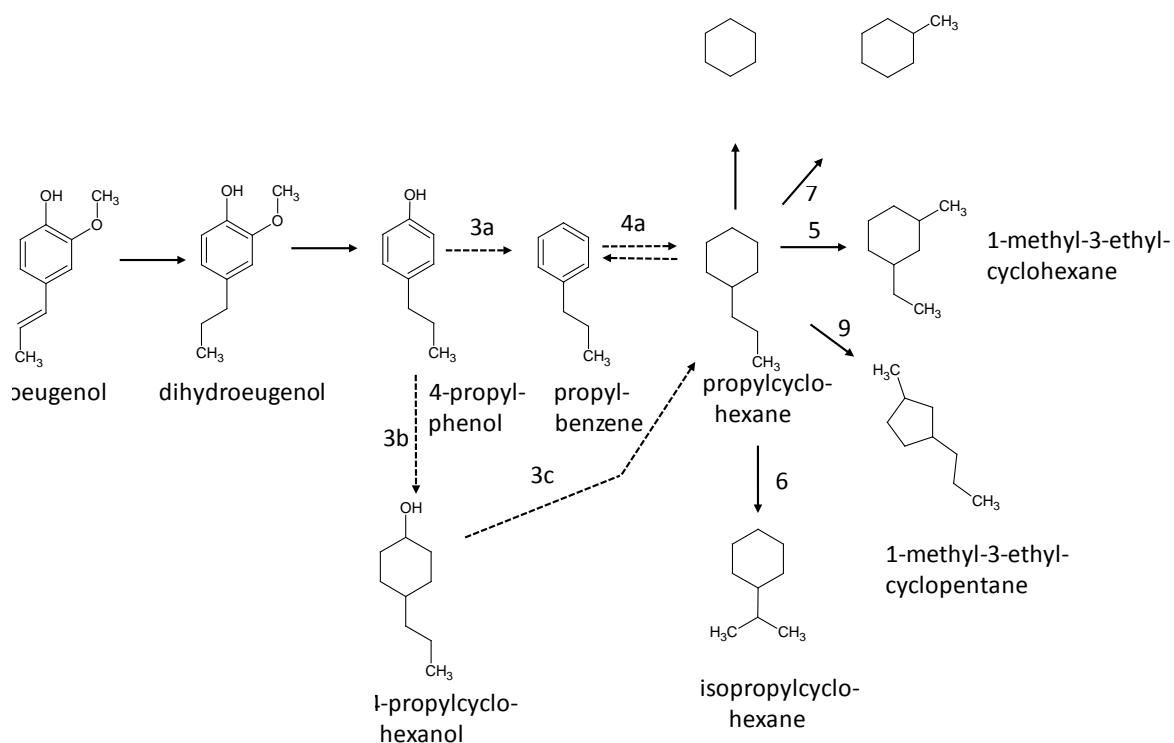
**Scheme 1.** Reaction scheme for isoeugenol hydrodeoxygenation.
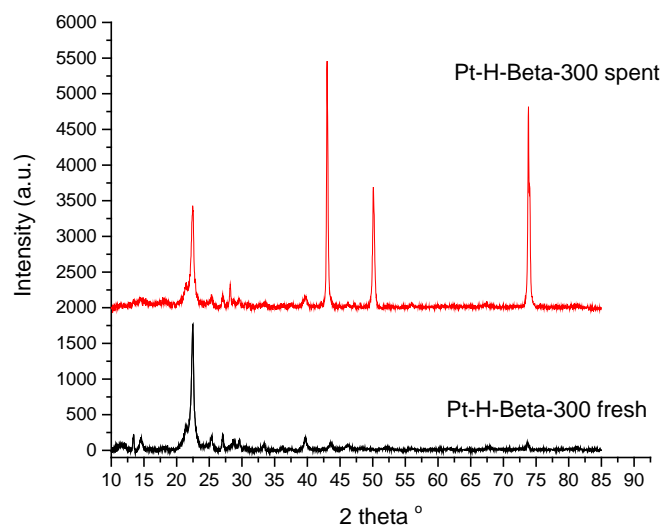
Figure 1. Diffractograms of the fresh and spent Pt-H-Beta-300. The peaks at 7.74, 13.44 22.47 and 27.07º correspond to the 101, 004, 302 and 008 Miller index planes on Beta zeolite. The Pt peaks at 2 theta 39.59, 46.2, 67.65 and 81.37º in the diffractogram correspond to Miller index planes of 111, 200, 220 and 311º, respectively. The peaks at 2 theta 43, 50.5 and 74º correspond to Cu from the sample holder in the diffractogram of the spent Pt-H-Beta-300.
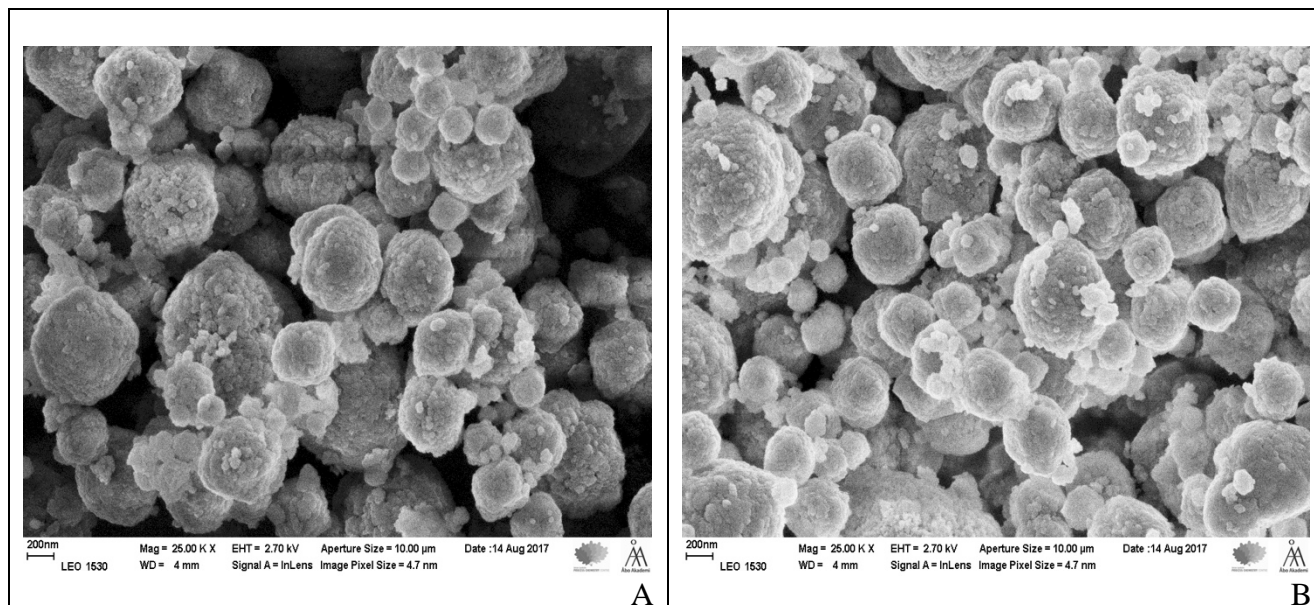
Figure 2. Scanning Electron Microscope images of a) fresh and b) spent Pt-H-Beta-300 catalyst after isoeugenol HDO at 200℃ and 3 MPa.
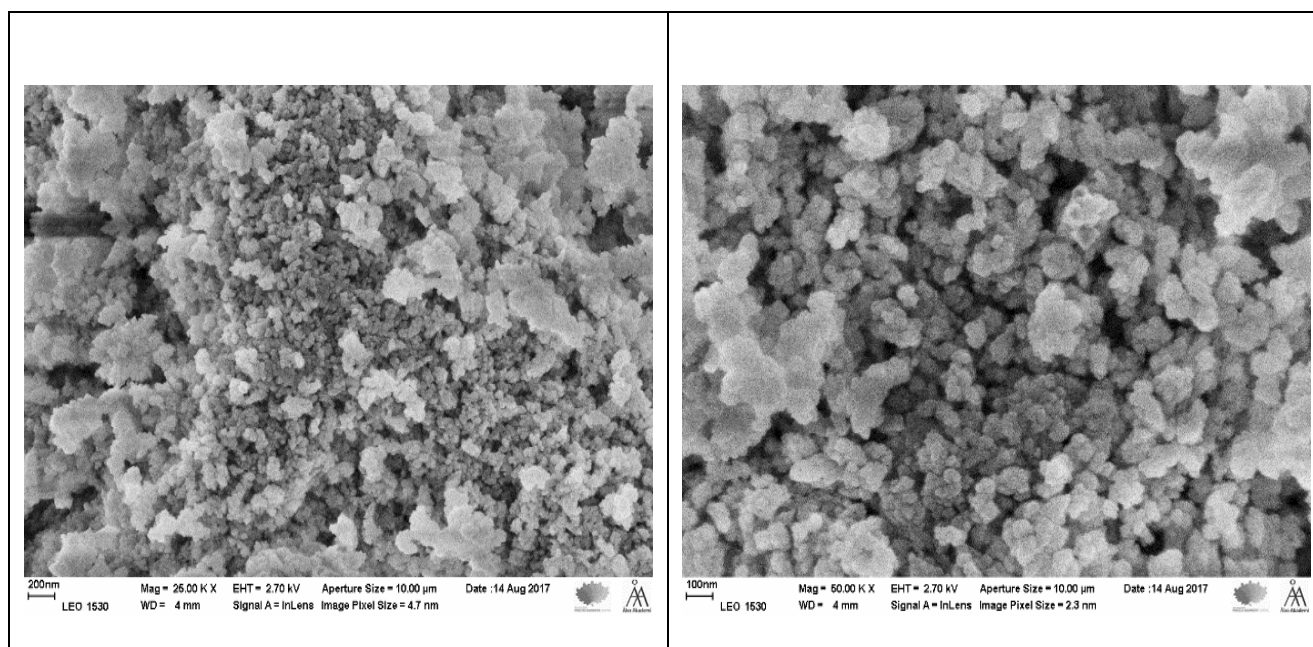
Figure 3. Scanning Electron Microscope images of fresh a) Pt-H-Beta-150 and b) Pt-H-Beta-25 catalysts.

31
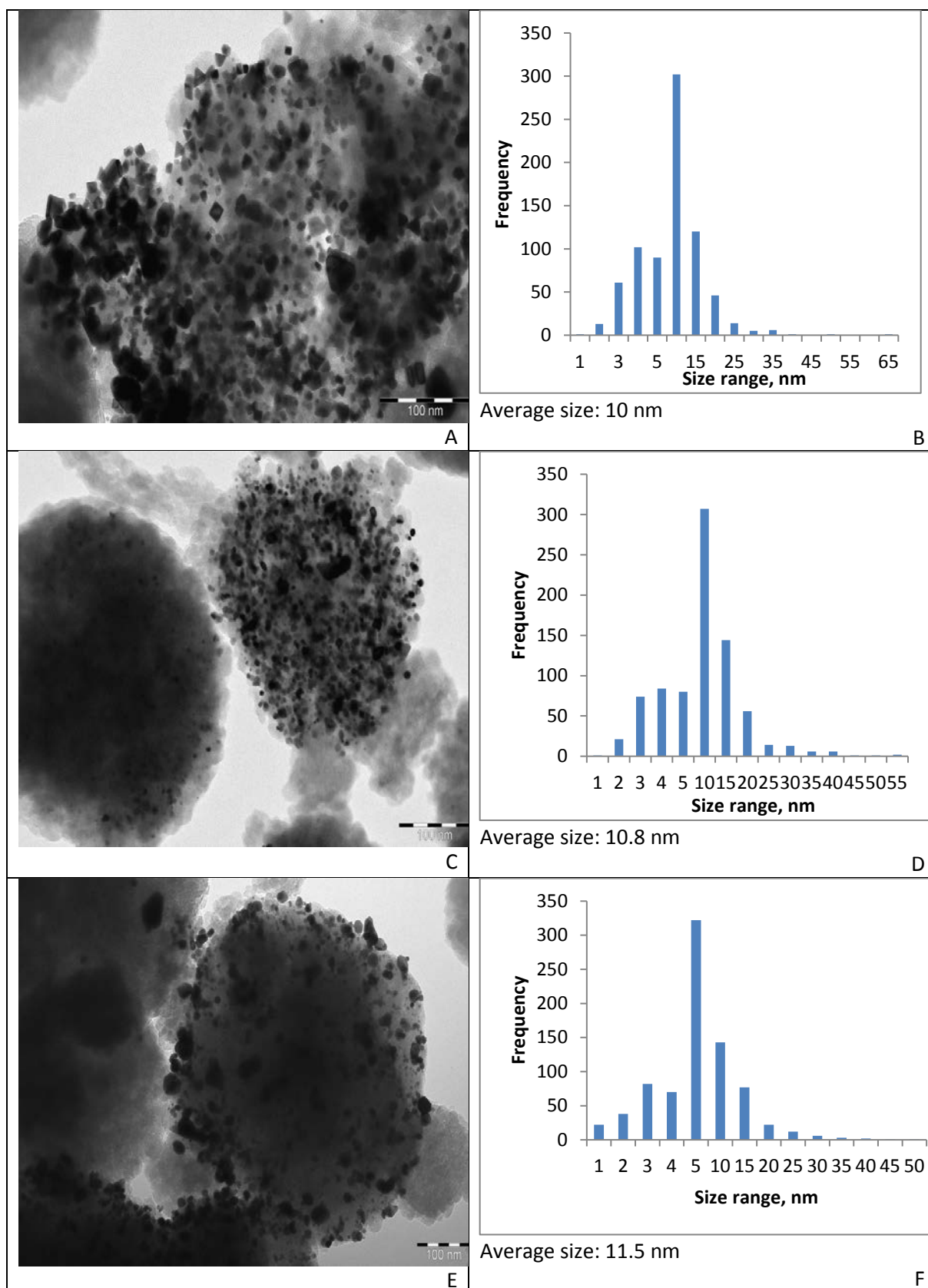
Figure 4. Transmission Electron Microscopy images and histograms of 2 wt% Pt-H-Beta-300 (fresh - A and B, spent – C and D, regenerated – E and F) in the reaction of isoeugenol at 200℃ and 3 MPa.
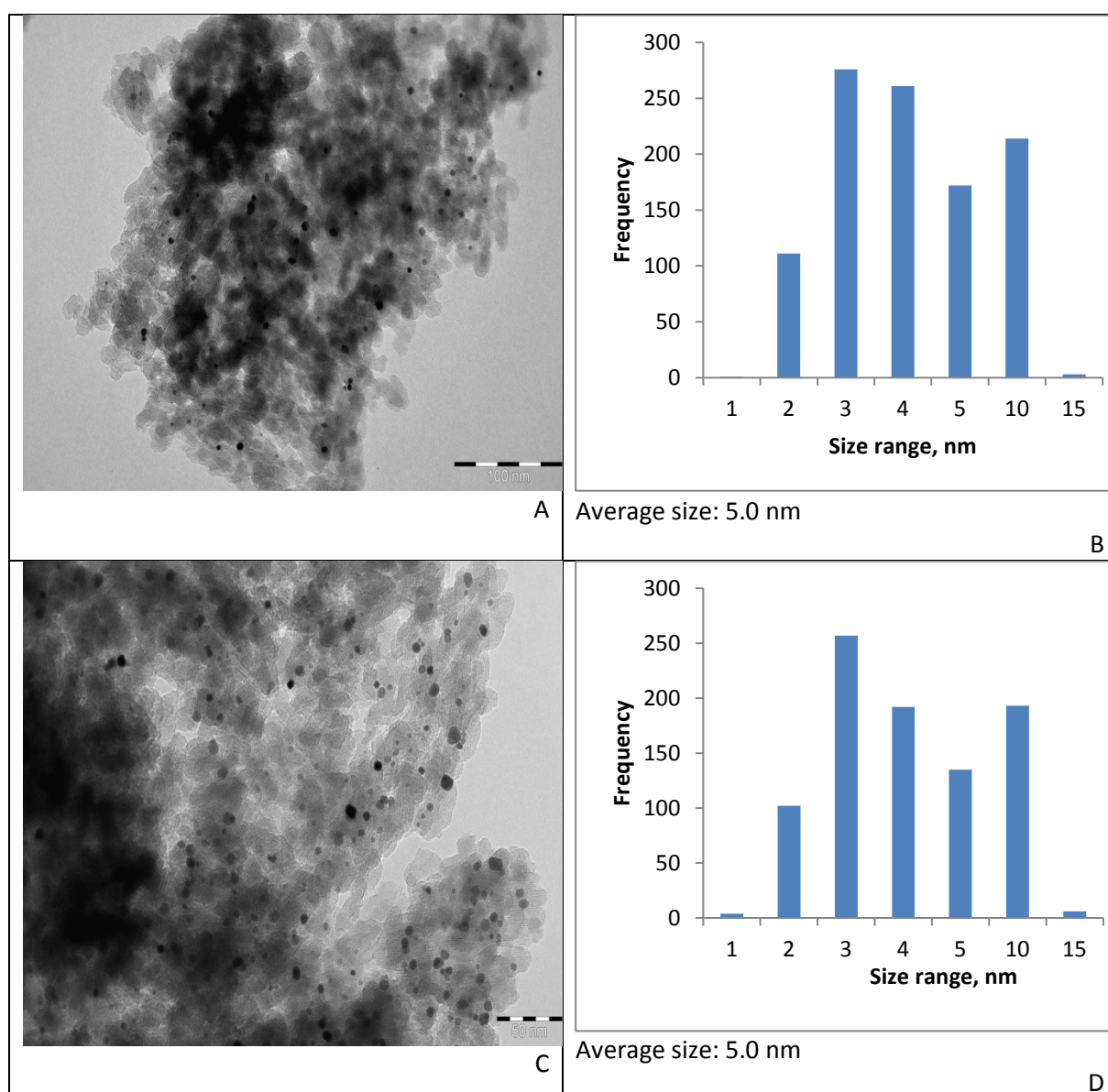
Figure 5. Transmission Electron Microscopy images and histograms of 1.2 wt% Pt-H-Beta-150 (fresh - A and B, spent – C and D) in the reaction of isoeugenol at 200℃ and 3 MPa.
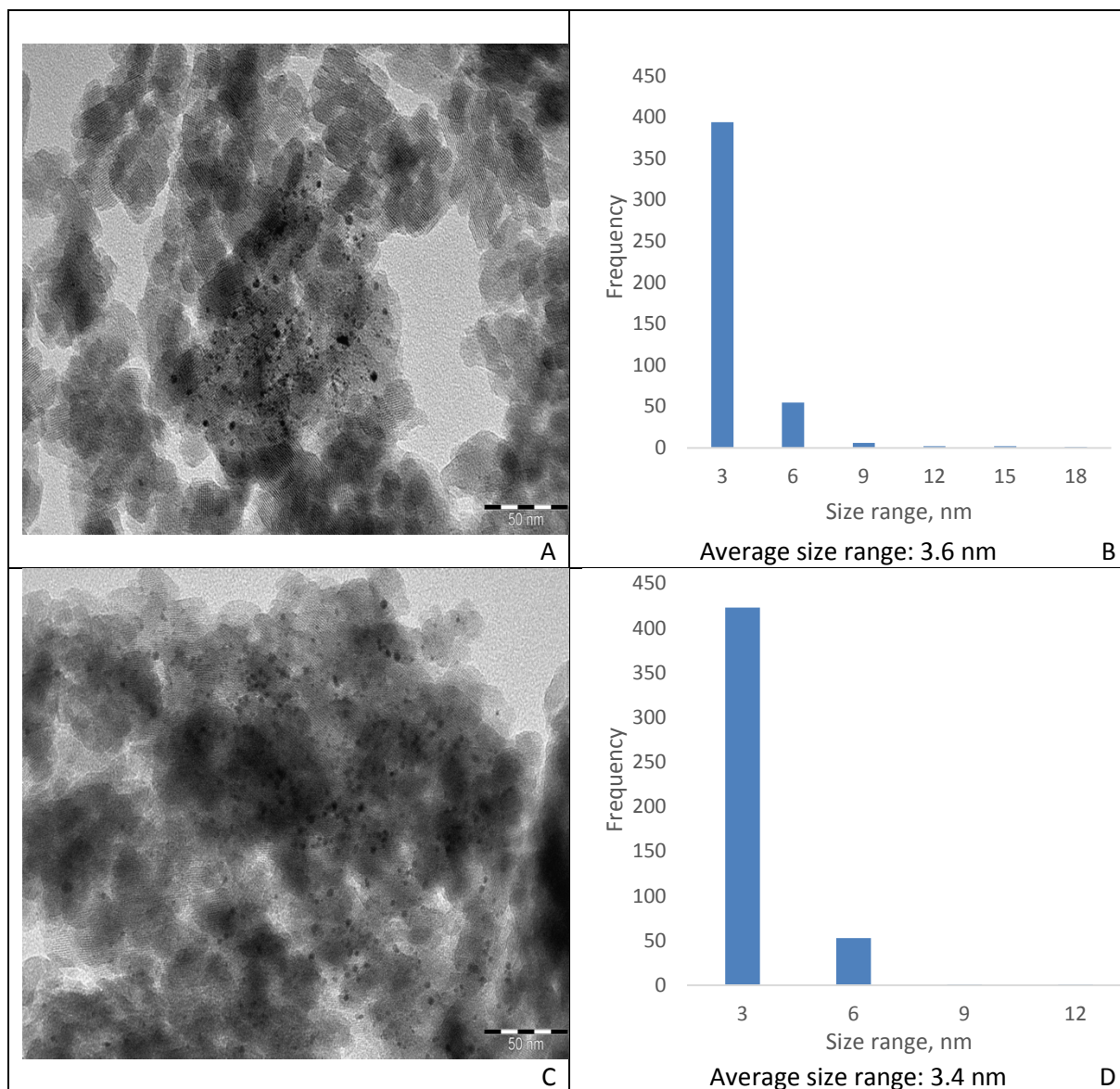
Figure 6. Transmission Electron Microscopy images and histograms of 2.5 wt% Pt-H-Beta-25 (fresh - A and B, spent – C and D) in the reaction of isoeugenol at 200℃ and 3 MPa.

34
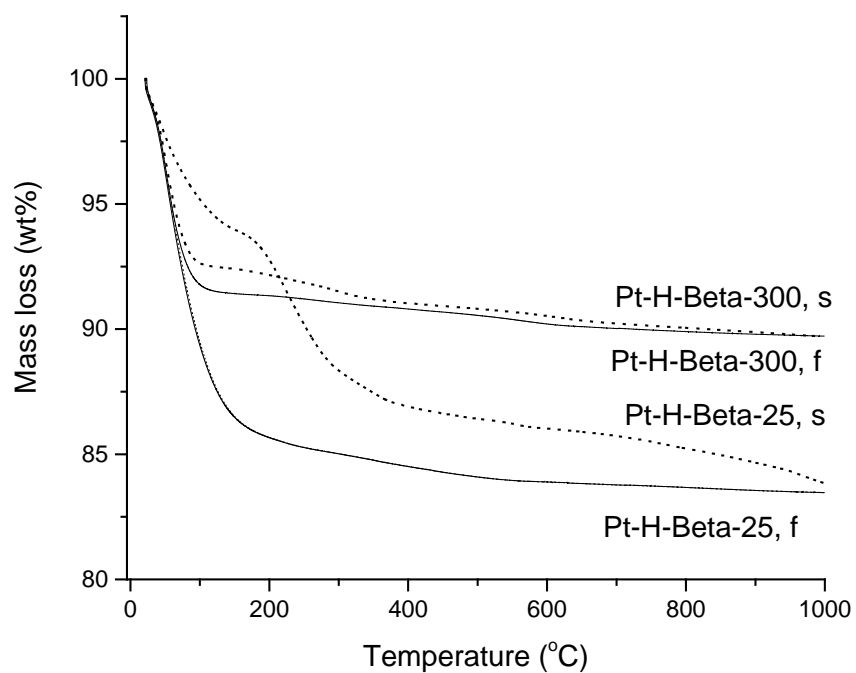
Figure 7. TGA of fresh (solid line) and spent (dashed line) Pt-H-Beta-300 and Pt-H-Beta-25.

a)

b)

36
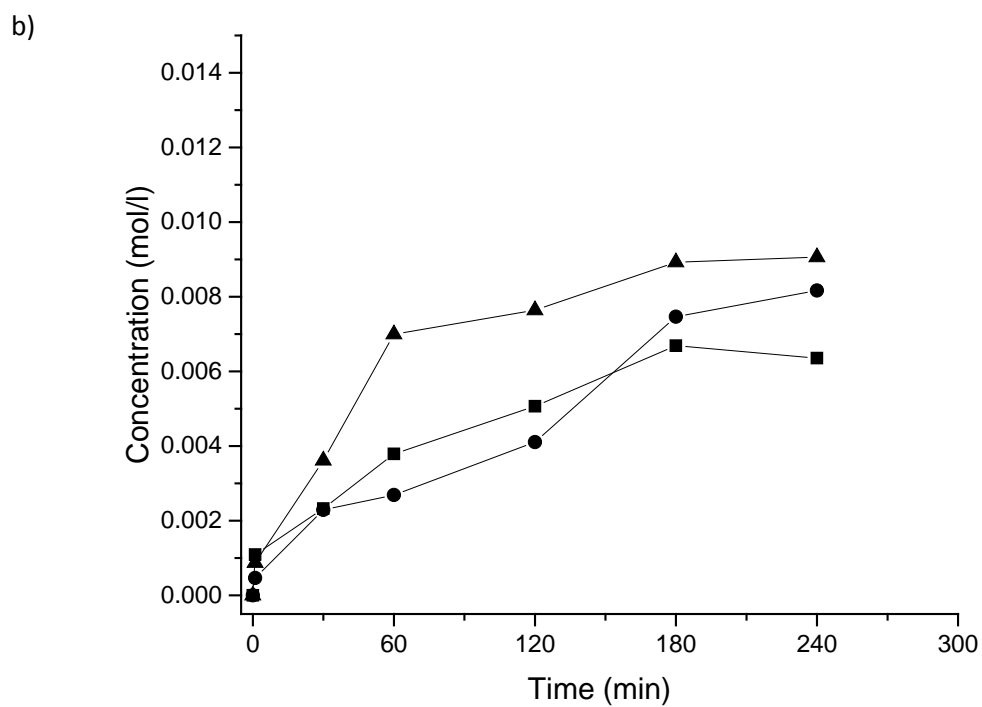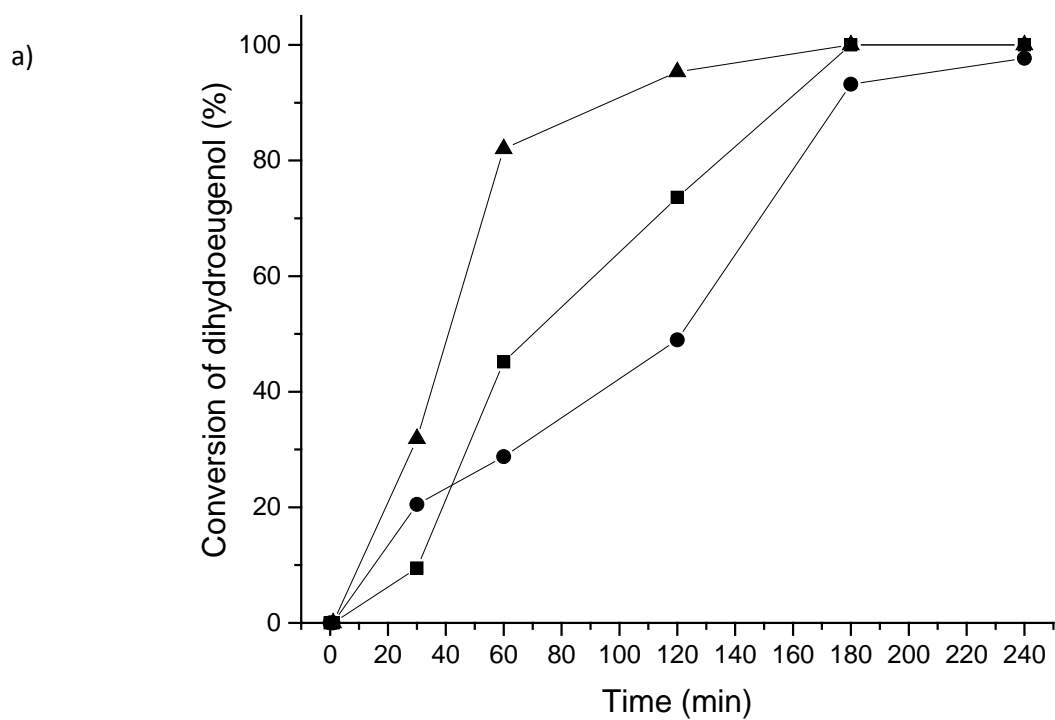
c)
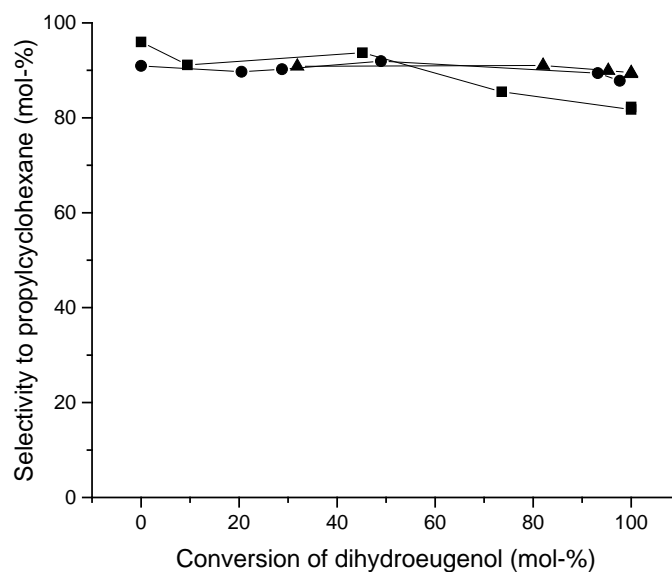
Figure 8. a) Conversion of dihydroeugenol, b) concentration of propylcyclohexane and c) selectivity to propylcyclohexane as a function of dihydroeugenol conversion in isoeugenol transformation over different Pt-Beta catalysts. Notation: Pt-Beta-300 (▲), Pt-Beta-150 (●) and Pt-Beta-25 (■). Conditions: initial concentration of isoeugenol 0.012 mol/l in dodecane, temperature 200°C total pressure 3 MPa, 50 mg catalyst.
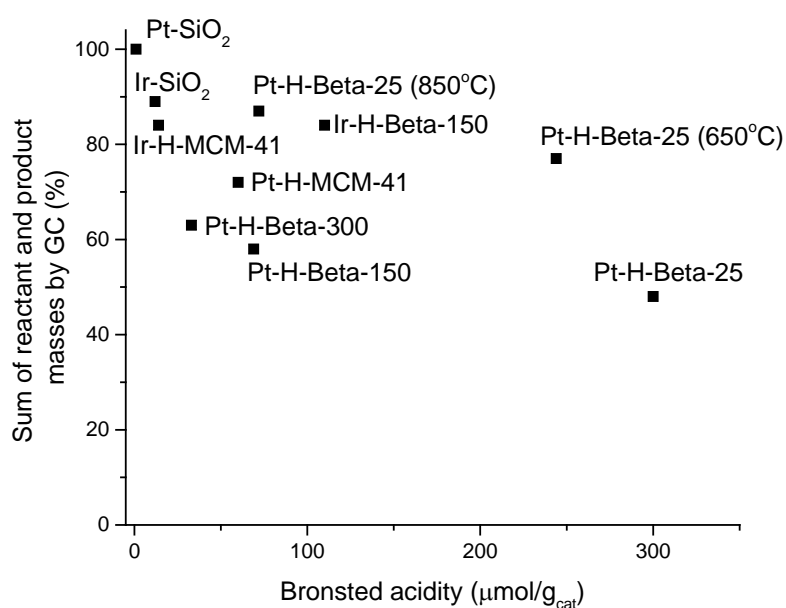

Figure 9. Sum of the liquid phase reactant and product masses as a function of the amount of Bronsted acid sites.
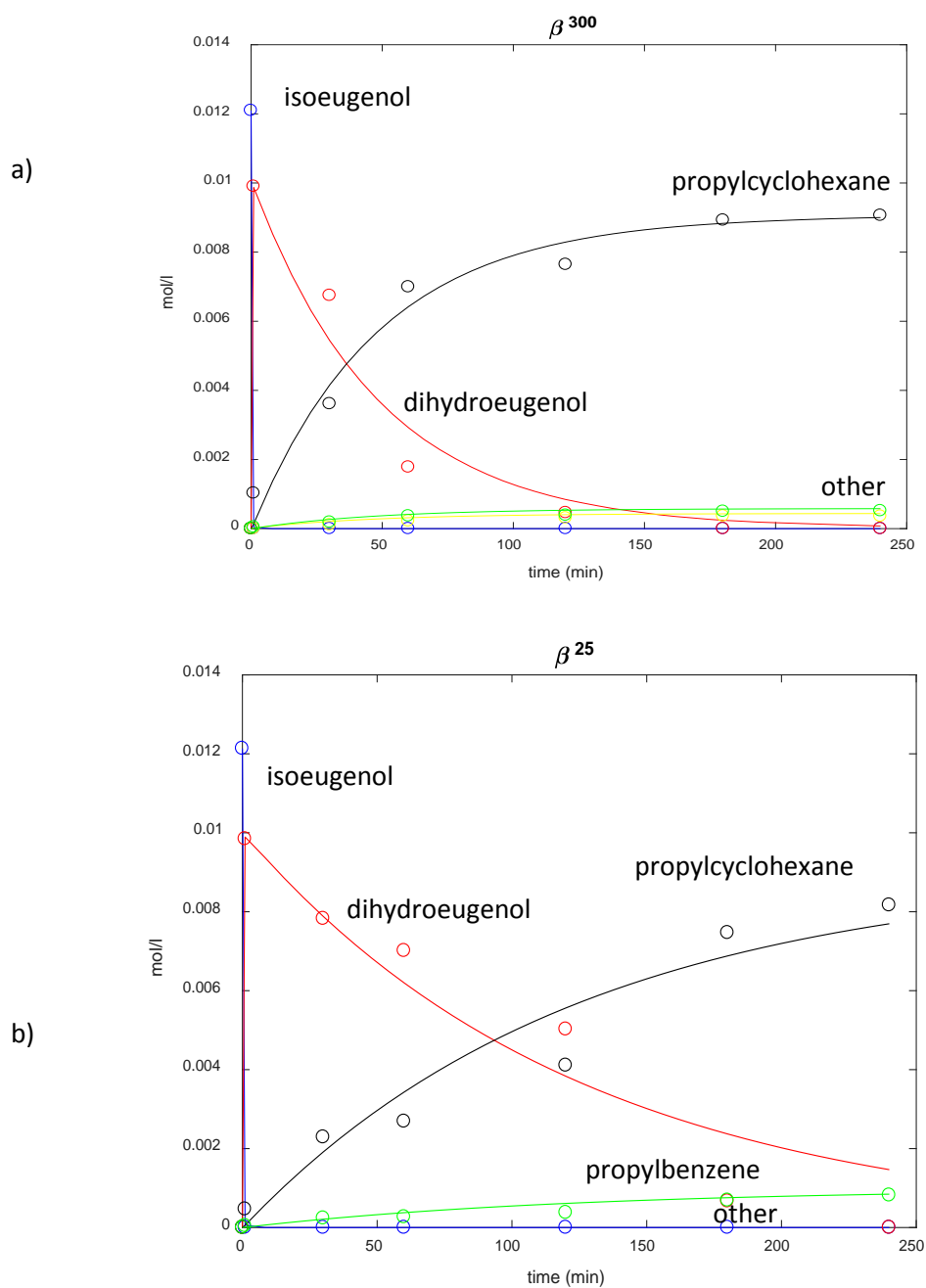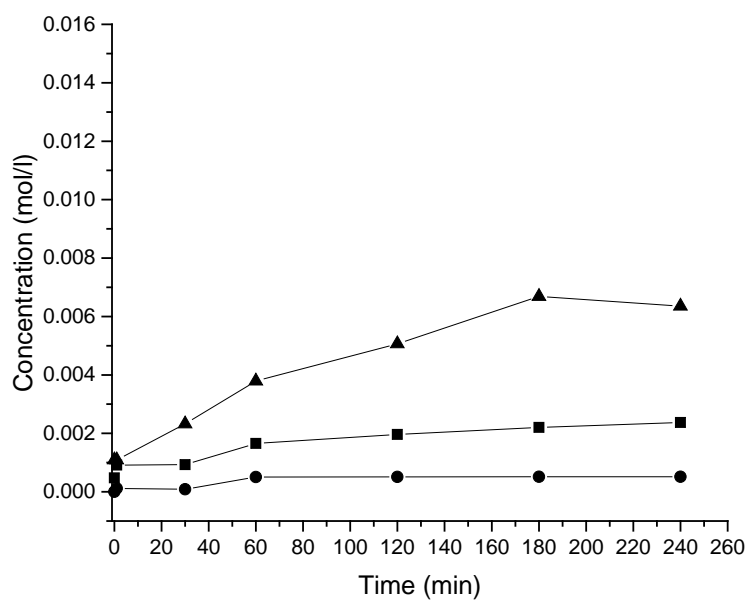
Figure 10. Kinetics of isoeugenol hydrodeoxygenation over a) Pt-H-Beta-300 and b) Pt-H-Beta-25 at 200°C under 3 MPa total pressure. Notation: points are experimental data and lines denote modelling. Conditions: initial concentration of isoeugenol 0.012 mol/l in dodecane, temperature 200ºC.
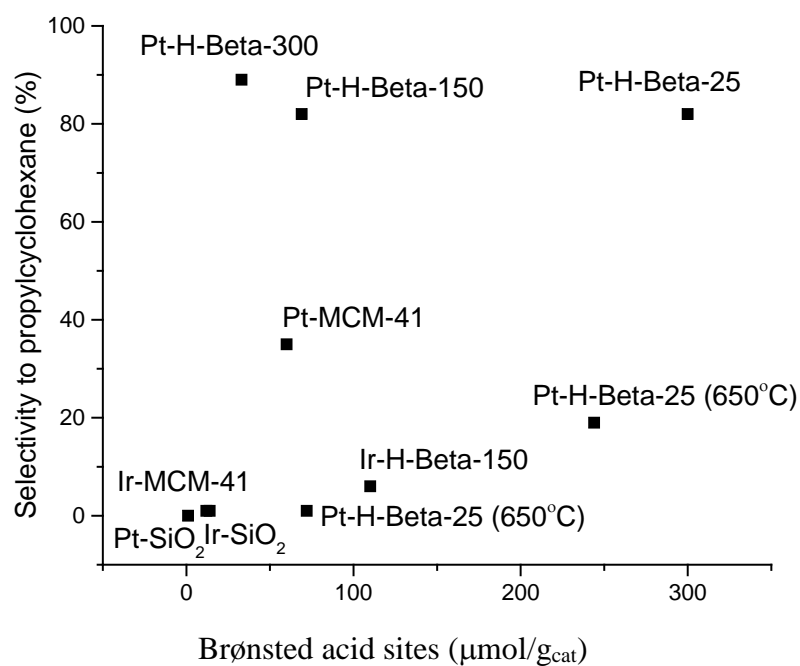
38

a)
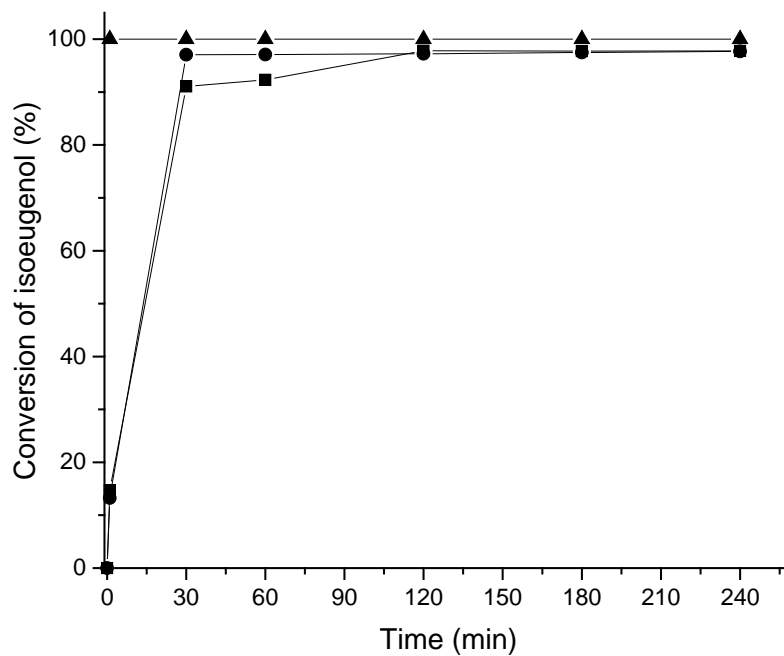
b)

Figure 11. a) Conversion of isoeugenol, b) Concentration of the formed propylcyclohexane in isoeugenol hydrodeoxygenation over Pt-H-Beta-25 calcined at 450°C (▲), 650 °C (■) and 850 °C (●). Conditions: initial concentration of isoeugenol 0.012 mol/l in dodecane, temperature 200°C total pressure 3 MPa.

39

Figure 12. Selectivity towards propylcyclohexane after 4h reaction in hydrodeoxygenation of isoeugenol at 200°C under 3 MPa total pressure as a function the amount of Brønsted acid sites.
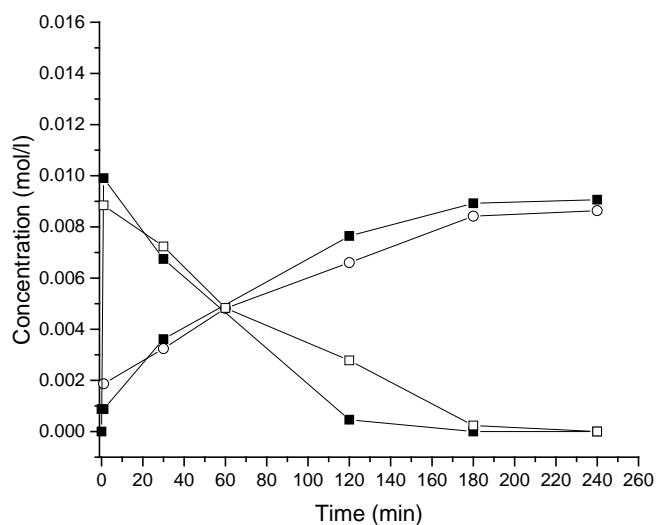
Figure 13. Hydrodeoxygenation of isoeugenol over fresh and regenerated Pt-H-Beta-300. Notations: Concentration of dihydroeugenol (■) and propylcyclohexane (●) as a function of time in hydrodeoxygenation of isoeugenol over fresh (open symbol) and spent, regenerated Pt-H-Beta-300 catalyst. Conditions: initial concentration of isoeugenol 0.012 mol/l in dodecane, temperature 200°C.
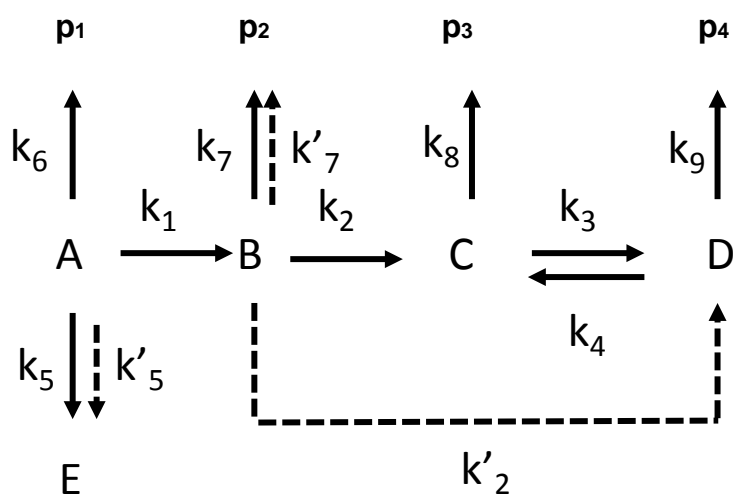
Figure 14. Reaction shceme used for modelling of the parameters in isoeugenol hydrodeoxygenation. Notation: A= isoeugenol, B= dihydroeugenol, C= propylbenzene, D= propylcyclohexane, E= isoeugenol dimer and side products p_1, p_2, p_3 and p_4. The dash lines denote a simplified reaction network , in which the intermediate C was not visible among the reaction products due to its fast reaction to D.

41

42

**Table 1.** Metal dispersion, metal particle size and specific surface areas of the tested catalysts.

Entry	Catalyst	Metal loading by EDX (%)	Metal dispersion (%)	Metal particle size by CO chemisorption (nm)	Metal particle size in fresh catalyst (nm)	Metal particle size in spent catalyst (nm)	Specific surface area (m^2/g_{cat})	Pore volume (cm^3/g_{cat})
1	Pt-H-Beta-300	1.98	13.1	8.6	10.0	10.8	686	0.24
2	Pt-H-Beta-150	1.20	15.2	7.5	5.0	5.0	621	0.22
3	Pt-H-Beta-25	2.49	17.6	6.5	3.4 (16.4[a], 29.5[b])	3.4	592	0.21
	Pt-H-Beta-300, 1. used	2.25	n.d.	n.d.	10.8	n.d.	681	0.24
	Pt-H-Beta-300, regenerated	n.d.	n.d.	n.d.	11.5	n.d.	650	0.23
4	Ir-H-Beta-150	0.67	2.1	51.2	25.2	-	n.d.	n.d.
5	Pt-H-MCM-41	2.42	11.7	9.7	30.9	25.6	679	0.45
6	Ir-H-MCM-41	1.71	4.2	25.4	[c]	[c]	n.d.	n.d.
7	1 wt% Pt/Al$_2$O$_3$ (Aldrich) [b]	n.d.	58.8	1.9	n.d.	n.d.	425	0.69
8	1 wt% Pt/SiO$_2$ [d]	n.d.	9.4	12.1	9	n.d.	341	0.72
9	1 wt% Ir/SiO$_2$ [d]	n.d.	n.d.	n.d.	5.8	-	390	0.63

catalyst calcined at [a] 650 °C and [b] 850°C were 6.9% and 3.8 % corresponding the Pt size of 16.4 nm and 29.5 nm, respectively, [c] varied a lot, [d] nominal loading, n.d. not determined

43

Table 2. The amount of Brønsted and Lewis acid sites determined by FTIR pyridine adsorption desorption method.

Catalyst	Brønsted acid sites (μmol/g$_{cat}$)			Lewis acid sites (μmol/g$_{cat}$)		
	250°C	350°C	450°C	250°C	350°C	450°C
Pt-H-Beta-300	33	2	0	12	5	0
Pt-H-Beta-150	69	3	0	17	9	3
Pt-H-Beta-25	300	16	0	88	2	0
Ir-H-Beta-150	110	87	0	53	16	0
Pt-H-Beta-25 (650°C)	244	17	0	62	2	0
Pt-H-Beta-25 (850°C)	72	0	0	43	1	1
Pt-H-MCM-41	60	5	0	55	12	0
Ir-H-MCM-41	14	5	0	55	12	0
1 wt% Pt/Al$_2$O$_3$	n.d.	n.d.	n.d.	n.d.	n.d.	n.d.
1 wt% Pt/SiO$_2$	1	1	0	3	1	0
1 wt% Ir/SiO$_2$	1	1	11	6	5	2

Accepted Manuscript

44

Table 3. Reactions used in thermodynamic analyses.

Accepted Manuscript

46

47
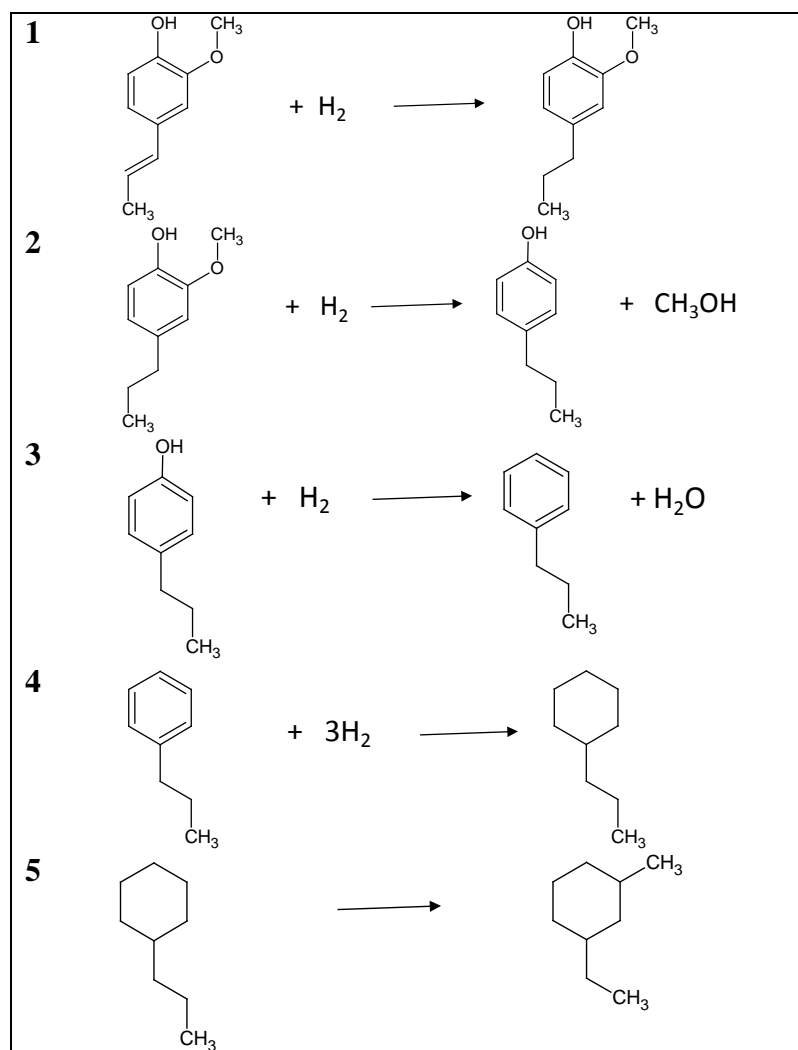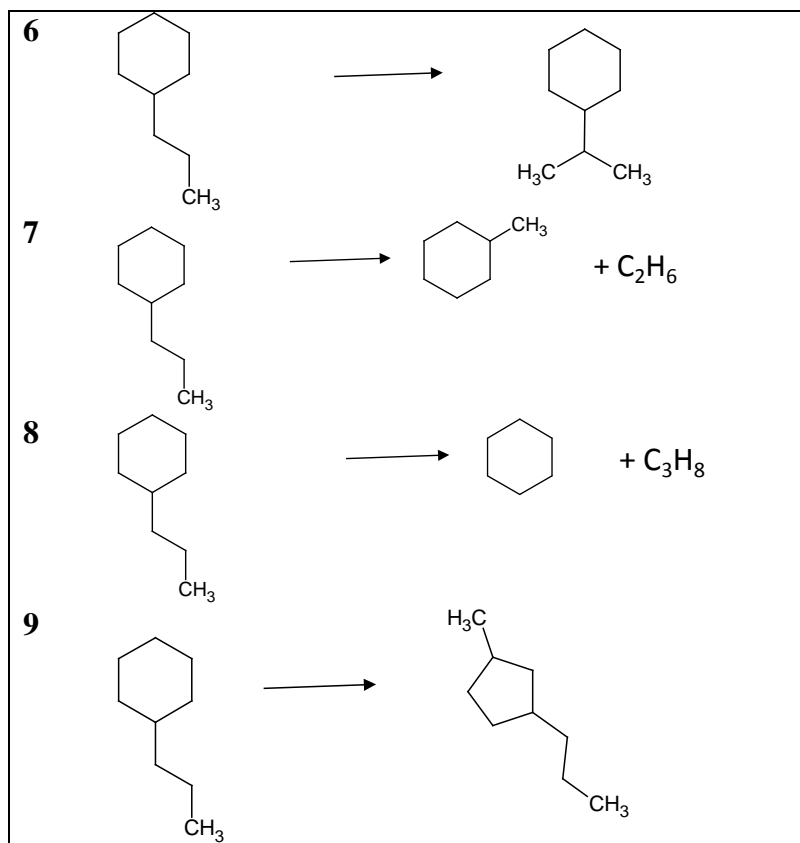
Table 4. The results from isoeugenol transformation in dodecane as a solvent over different catalysts. Conditions: 200°C, total pressure 3 MPa, initial isoeugenol concentration 0.012 mol/l if not else stated.

Entry	Catalyst	TOF (s^{-1})[a]	Conversion of dihydroeugenol after 4 h (%)	Sum of liquid phase masses of reactant and product determined by GC (%)	Main product	Selectivity to main product after 4 h (%)	Selectivity to the second main product after 4 h (%)
1	Pt-H-Beta-300	0.17	100	61 (63[b])	propylcyclohexane	89	1-methyl-2-propyl-cyclohexane, 6
2	Pt-H-Beta-150	0.15	98	58	propylcyclohexane	82	1-methyl-4-ethylcyclohexane[c], 10
3	Pt-H-Beta-25	0.07	100	45 (48[b])	propylcyclohexane	82	1-methyl-4-ethylcyclohexane[c], 12
4	Ir-H-Beta-150	0.14	3	84	dihydroeugenol	82	1-methyl-2-propylcyclohexane[d], 6
5	Pt-H-Beta-25 (650°C)	n.d.	98	77	dihydroeugenol	78	Propylcyclohexane, 19
6	Pt-H-Beta-25 (850°C)	n.d.	32	87	dihydroeugenol	99	Propylcyclohexane, 1
7	Pt-H-MCM-41	0.02	46	72	dihydroeugenol	63	Propylcyclohexane, 35
8	Ir-H-MCM-41	0.07	1	84	dihydroeugenol	99	Propylcyclohexane, 1
9	Pt/Al$_2$O$_3$	0.004	4	100	dihydroeugenol	99	Trimethylbenzene, 1
10	Pt/SiO$_2$	0.004	1	100	dihydroeugenol	99	Trimethylbenzene, 1
11	Ir/SiO$_2$[a]	n.d.	9	89	dihydroeugenol	99	Propylcyclohexane, 1
12	Pt-H-Beta-300, regenerated, reuse	n.d.	100	61	propylcyclohexane	89	Ethyl-methylcyclohexane[c], 9.5

[a] initial TOF for transformation of dihydroeugenol calculated by dividing the moles of the converted dihydroeugenol by moles of Pt and time during the first 30 min, [b] addition of organic material calculated from TGA to GC mass balance , [c] or another dialkylated cyclohexane with nine carbon atoms, identification made by GC-MS

Table 5. Parameter values in kinetic modelling of isoeugenol hydrogeoxygenation under 3 MPa total pressure in hydrogen at 200°C over Pt-H-Beta-300 and Pt-H-Beta-25.

Catalyst Pt-H-Beta-300				Catalyst Pt-H-Beta-25			
parameter	Estimated value	Estimated std. error	Estimated relative std. error (%)	parameter	Estimated value	Estimated std. error	Estimated relative std. error (%)
k_1	4.86	0.055	1.1	k_1	4.37	7.04	161.1
k_2	0.0195	0.0012	6.0	k'_2	0.0072	$0.556 \cdot 10^{-3}$	7.7
k_3	14.1	0.543	3.8	k'_5	0.93	1.61	172.9
k_4	0.684	0.022	3.2	k'_7	$0.789 \cdot 10^{-3}$	$0.277 \cdot 10^{-3}$	47.8
k_5	0.98	0.0050	0.5				
k_7	0.0012	$0.66 \cdot 10^{-4}$	5.6				

50

51